

ELECTRIC CURRENTS IN THE IONOSPHERE IN THE
REGIONS OF THE HIGHER LATITUDES

BY

ANNICK MENDEL

(Thesis to obtain the Diplome of Etudes Superieure
of Physics)

From: Centre National d'Etudes des Telecommunications, Groupe de Recherches
Ionospheriques, Note Technique GRI/NT/63, December 1966.

Translated by
Belov & Associates
for
N.A.S.A. GSFC Library
Contract NAS 5-10888
Item no. 10888-030
December 1969

FACILITY FORM 602

N70-73731

(ACCESSION NUMBER)

(THRU)

42
(PAGES)

None
(CODE)

CR-110111
(NASA CR OR TMX OR AD NUMBER)

(CATEGORY)



CONTENTS

<u>Introduction</u>	1
<u>Chapter 1 Definitions and notations</u>	2
1. The earth's magnetic field	2
2. Average of several vectors	2
3. Indexes	3
4. Laws of regression	3
5. Field-current relation	6
<u>Chapter 2 Calculation of the undisturbed field H_0</u>	9
1. Method using the calmest hours and days	9
2. Hodograph method	11
3. Comparison of the two methods	13
<u>Chapter 3 Study of the density vector of current i</u>	16
1. Study of the intensity of the density of current i	16
2. Study of the direction of the density vector of current i	19
<u>Chapter 4 Study of I</u>	24
1. Calculation of the I effect of an error of origin	24
2. Comparison of the values of I for different stations	25
3. Evidences of the seasonal variation	27
4. Comparison of I to A_p	28

CONTENTS
(Continued)

<u>Conclusion</u>	31
<u>Appendix 1</u>	33
<u>Appendix 2</u>	35

INTRODUCTION

This study will be conducted on the ionospheric currents in high latitude regions. Average hourly values of the components of the earth's magnetic field will be used. These values were calculated from records taken from polar stations, particularly during the International Geophysic Year. (fig. 1).

From the data given, it will be shown how information on the average hourly values \vec{i} of the densities of current at the zenith of the stations utilized can be obtained. The properties of the \vec{i} vector will be studied. The I parameter, average of the 24 hourly values of $|\vec{i}|$ for a given day, was introduced by Lebeau (1965). This will be calculated and his correlations with A_p will be studied for different stations.

The density of the zenithal current \vec{i} from average hourly values of the horizontal components of the total magnetic field will be arrived at in the first stage of this paper. It will be necessary therefore to state the relation between the density of the current and a field disturbance and to calculate the value of an undisturbed field, i.e., the value which will occur for nul \vec{i} .

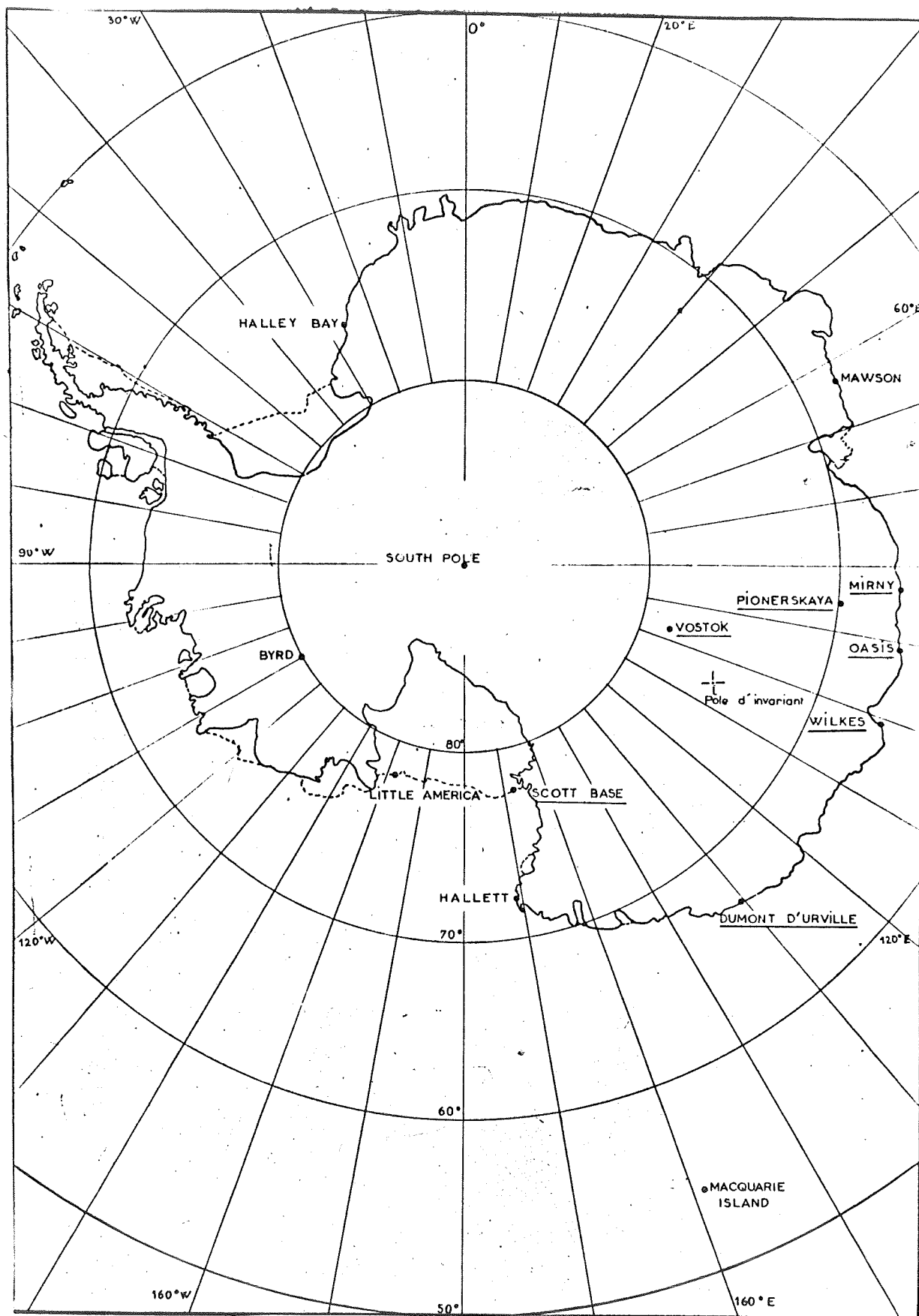


Fig. 1 Positions of the Antarctic stations studied.

Station	1 Symbole	2 Latitude géographique	3 Colatitude magnétique	4 L. heure du midi local	5 M. heure du midi magnétique	M - L
VOSTOK	Vo	78° 27' S	5.50	4.88	13.03	+ 8.15
DUMONT D'URVILLE	DU	66° 40' S	9.48	2.67	1.17	- 1.50
WILKES	WK	66° 25' S	9.83	4.64	6.08	+ 1.44
SCOTT BASE	SB	77° 51' S	10.04	0.88	19.19	- 5.69
PIONEERSKAYA	PO	69° 44' S	10.19	5.63	8.76	+ 3.13
OASIS	OA	66° 16' S	11.61	5.29	7.38	+ 2.09
MIRNY	MI	66° 33' S	13.18	5.80	8.26	+ 2.46
HALLETT	HE	72° 18' S	12.71	0.65	21.00	- 3.65
LITTLE AMERICA	LA	78° 16' S	16.13	22.81	18.54	- 4.27
THULE	TH	77° 29' N	3.56	16.61	13.83	- 2.78
GODHAVN	GO	69° 14' N	12.88	15.57	13.87	- 1.70

Table 1 Values of the principle parameters relative to the stations studied.

Table 1 legend: 1- Symbol; 2- Geographic latitude; 3- Magnetic colatitude; 4- Local time from local noon; 5- Magnetic time from magnetic noon

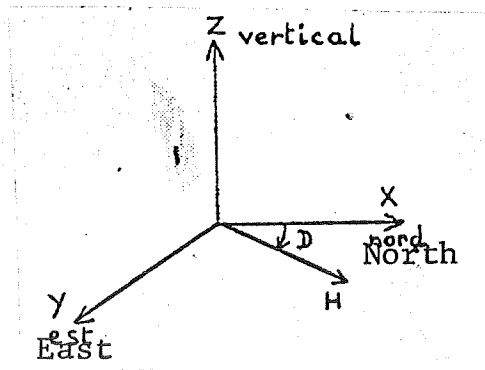


Fig. 2 Components of the magnetic field

CHAPTER 1

Definitions and notations

1. The Earth's magnetic field:

Three components of the earth's magnetic field are recorded in a coninum by several observatories (fig. 2):

-either the North, East and vertical components, whose hourly average values will be assigned X_i, Y_i, Z_i , where i designates the hourly interval of universal time,

-or the intensity of the horizontal field, the declination and the vertical component, whose average hourly values will be assigned H_i, D_i, Z_i .

The stations whose data were used provided H, D , and Z , except in the cases of Dumont d'Urville (DU) and Scott Base (SB). The average hourly values of H_i and D_i were systematically converted to rectangular components before calculating the arithmetic averages. However rigorously applied, this system does not lead to the average hourly value which would be derived from instant values of rectangular components; it is felt, however, that the approximation obtained is sufficient.

2. Average of several vectors:

The vector \vec{V}_0 , the average of $n \vec{V}_j$ coplanary:

-either by its co-ordinates in a diagram related to the

rectangular axes \vec{X} and \vec{Y} :

$$Y = \frac{1}{n} \sum_{j=1}^n Y_j \quad X = \frac{1}{n} \sum_{j=1}^n X_j$$

-or by its extremity P, barycenter of the extremities P_j of the vectors \vec{V}_j ($\vec{OP} = \vec{V}$).

3. Indexes

Except for specifications to the contrary, the following will be used:

- from the index 0, values relative to the undisturbed fields,
- from the i and j indexes, values relative to the i^{th} hourly interval of the j^{th} day in the year,
- from the j index only, the values relative to the averages made over the 24 hourly intervals of the j^{th} day,
- from the i index only, the values relative to the i^{th} hourly interval, averaged over a group of defined days.

4. Laws of Regression:

In the course of this study, the relations that exist between the observed X and Y magnitudes, looking for the law which best describes the points representative of the observations in a rectangular diagram where one of the magnitudes X is assigned to the abscissa and the other, Y, to the ordinate, will be made precise. Methods of adjustment of the law to the points of the different observations will be used according to the nature of

the magnitudes to be compared.

The co-ordinates of the points observed in the diagram, X_r , Y_r , will be assigned to the rectangular axes \vec{X} , \vec{Y} , whose origin is taken at the barycenter O of the points of observation.

First case:

X_r is a known quantity, whereas the differences between Y_r from the unknown straight line are considered as uncertainties of measurement. The straight line of the least squares in Y will be traced, i.e., the straight line so that the average quadratic difference is minimal (fig. 3).

$$\frac{1}{n} \sum_{r=1}^n (Y_r - Y(X_r))^2$$

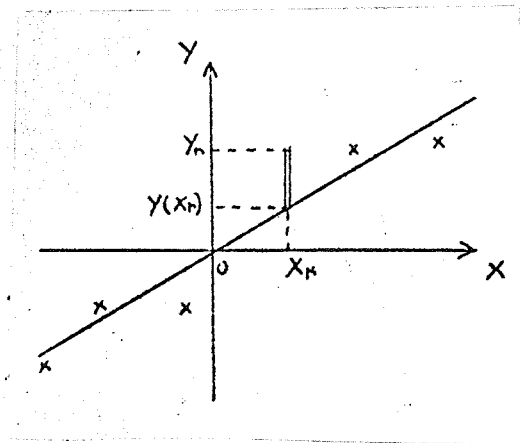


Fig. 3 Straight line of the least squares in Y .

The calculation of the coefficients of this straight line is classic,

-it goes through the barycenter O of the points

-its slope is

$$a = \frac{\sum X_r Y_r}{\sum X_r^2}$$

-moreover, the coefficient of correlation is introduced

$$R = \sqrt{1 - \frac{\sum (Y_r - Y(X_r))^2}{\sum Y_r^2}}$$

Second case: X_r and Y_r are affected by uncertainties of the same order and are relative to magnitudes of the same order. The straight line of the least distances, which is such that the sum of the squares of the Eculidian distances of the points (X_r, Y_r) (fig. 4) $\sum dr^2$ minimal, will be drawn.

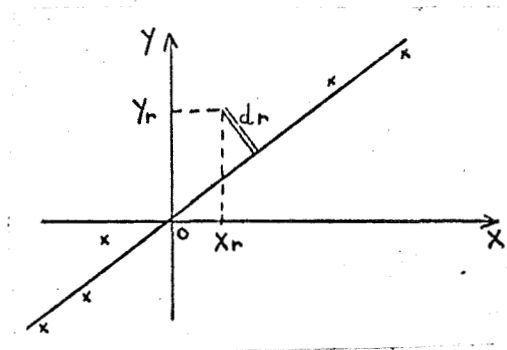


Fig. 4 Straight line of the least distances

It will be demonstrated that it passes through the barycenter of the points. The calculation of its slope "a" leads to the relation:

$$a = - \frac{\sum X_r^2 - \sum Y_r^2}{2 \sum X_r Y_r} + \sqrt{\left(\frac{\sum X_r^2 - \sum Y_r^2}{2 \sum X_r Y_r} \right)^2 + 1}$$

(Annex 1)

A coefficient of correlation analagous to the one defined for the straight line of the least squares will be introduced.

$$R = \sqrt{1 - \frac{\sum dr^2}{\sum (X_r^2 + Y_r^2)}}$$

In certain cases, the straight line of the least distances passing through a fixed point other than the barycenter will be used.

Third case: X_r and Y_r are affected by uncertainties of the same order, but they are relative to magnitudes of a different nature. The Euclidian distance from a point (X_r, Y_r) to a straight line, in the diagram (\vec{X}, \vec{Y}) no longer has any significance. In fact, a change of unity for one of the magnitudes corresponds to an affinity parallel to one of its axes, i.e., a geometric transformation that does not stay perpendicular. The straight line of the least squares in Y and of the least squares in X will be looked for. If these two straight lines have neighboring coefficients, the relation will be described by one or the other of these straight lines. If they have very different coefficients, representation by a linear relation will be considered impossible.

5. Field-current relation:

In order to pass from the disturbance of the field to the density of the zenithal current, which is supposed to bring it about, a certain number of hypotheses are indispensable. On one hand, it is admitted that the effect of distant currents can be ignored compared with that of the currents that circulate in the ionosphere at the level of the E region and in the vicinity of the station. This hypothesis is not unanimously accepted, but it generally is accepted to interpret polar disturbances. On

the other hand, the effect of gradients in the density of the current is ignored and it is admitted that the disturbances created at ground level correspond to the effect of a sheet of uniform and infinite current, having the density at the aplomb of the station for its density. This hypothesis would not be acceptable in the vicinity of an electrojet, but it is acceptable in the central region of the polar cap where \vec{i} does not present very acute local gradients. Finally the effect of currents induced in the ground can be ignored. Note that this effect is very complicated. It depends in particular on the nature of the subsoil and on the period of the phenomenon being studied. However, it affects the average hourly values of any one station in a rather uniform way, and modifies the vertical component above all. It is admitted that in a homogeneous soil the effect is that the modulus of the field created by a k factor greater than 1 (Chapman, 1940; Fairchild, 1963) is multiplied. The effect of inhomogeneities of the subsoil will be ignored and the k value, which will be presumed to be the same in all the stations, will not be specified.

Averaging these hypotheses, \vec{i} and the disturbance $\vec{\Delta H}$ are bound by a simple local relation; $|\vec{\Delta H}|$ is proportional to $|\vec{i}|$ and the direction of the vector $\vec{\Delta H}$ is deduced from that of $|\vec{i}|$ by a rotation of $+\frac{\pi}{2}$ (Fig. 5).

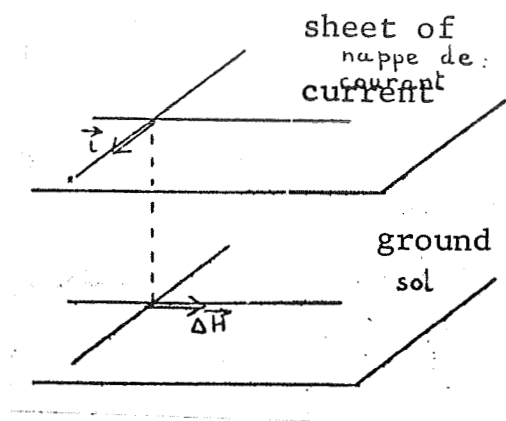


Fig. 5 $\vec{\Delta H}$ disturbance created by a sheet of current of a density of \vec{i} .

γ will be used to express \vec{i} . A density of current of 1γ created by a disturbance of 1 by definition.

Note that gamma (γ) is a unity of magnetic field equal to 10^{-5} oersted, i.e., in unity S.I.

$$1\gamma = 10^{-5} \times \frac{1}{4\pi \cdot 10^{-3}} \text{ A/m.}$$

Given that the relation between the sheet of current and the field created establishes S.I. in unity, is $\vec{\Delta H} = \frac{\vec{i}}{2}$, it is easily seen that:

$$i = 1\gamma = 1.59 \text{ A/km.}$$

CHAPTER 2

Determination of the undisturbed \vec{H}_0 field

In order to determine \vec{H}_0 two different methods were used, both based on houristic hypotheses; they led to similar results.

1. Method using the calmest hours and calmest days:

An attempt will be made to select hours during which the undisturbed field is directly observed, i.e., for which the zenithal current is negligible. Toward this end, the hourly interval which, for the group of days in 1958 corresponds to the weakest dispersion of the \vec{H}_{ij} vectors, will be determined for each station. The quantity:

$$Eq_i = \frac{1}{n} \sum_{j=1}^n |\vec{H}_{ij} - \vec{H}_i|$$

(n = 365 if no observation is missing)

will define the H_{ij} vector dispersion. Making the hypothesis that Eq_i and $|\vec{H}_i - \vec{H}_0|$ are minimum at the same time, the undisturbed field can be determined as an average, taken on the calmest days, some field vectors corresponding to this hourly interval. This value will be noted \vec{H}_{01} (X_{01} , Y_{01} , P_{01}).

1.1 Daily variation of Eq_i :

This calculation was made for two Arctic stations (Godhavn (GO) and Thule (Th)) and for eight Antarctic stations of magnetic

colatitude inferior to 14° whose magnetic activity was studied by Lebeau (1965): (Vostok (Vo), Dumont D'Urville (DU), Wilkes (Wk), Scott Base (SB), Pioneerskaya (Po), Mirny (Mi), Hallet (Ht)).

For each of the stations the representative curve of E_{q_i} as a function of the hourly interval (fig. 6) presents a unique maximum whose H_a hour is close to that of local noon L . The values of H_a and of the hourly interval corresponding to the minimum are assembled in table 2.

The law of regression of H_a in function of L gives the following equation (fig. 7):

$$\underline{H_a = 1.097 L - 0.529 \text{ hour}}$$

$$\text{Coefficient of correlation} \quad \underline{0.968}$$

$$\text{Average quadratic difference} \quad \underline{0.563 \text{ hour}}$$

The value of the ordinate at the origin is less than that of the average quadratic difference and the slope of the law of regression is in proximity to 1; it may be concluded, therefore, that the dispersion of the \vec{H}_{ij} vectors is maximal at local noon:

$$\underline{H_a = L}$$

Lebeau (1965), studying the magnetic activity characterized by the K indexes yields a very different result; the magnetic activity is in fact maximal at an H hour equidistant from local noon and magnetic noon:

$$\underline{H = \frac{M+L}{2}}$$

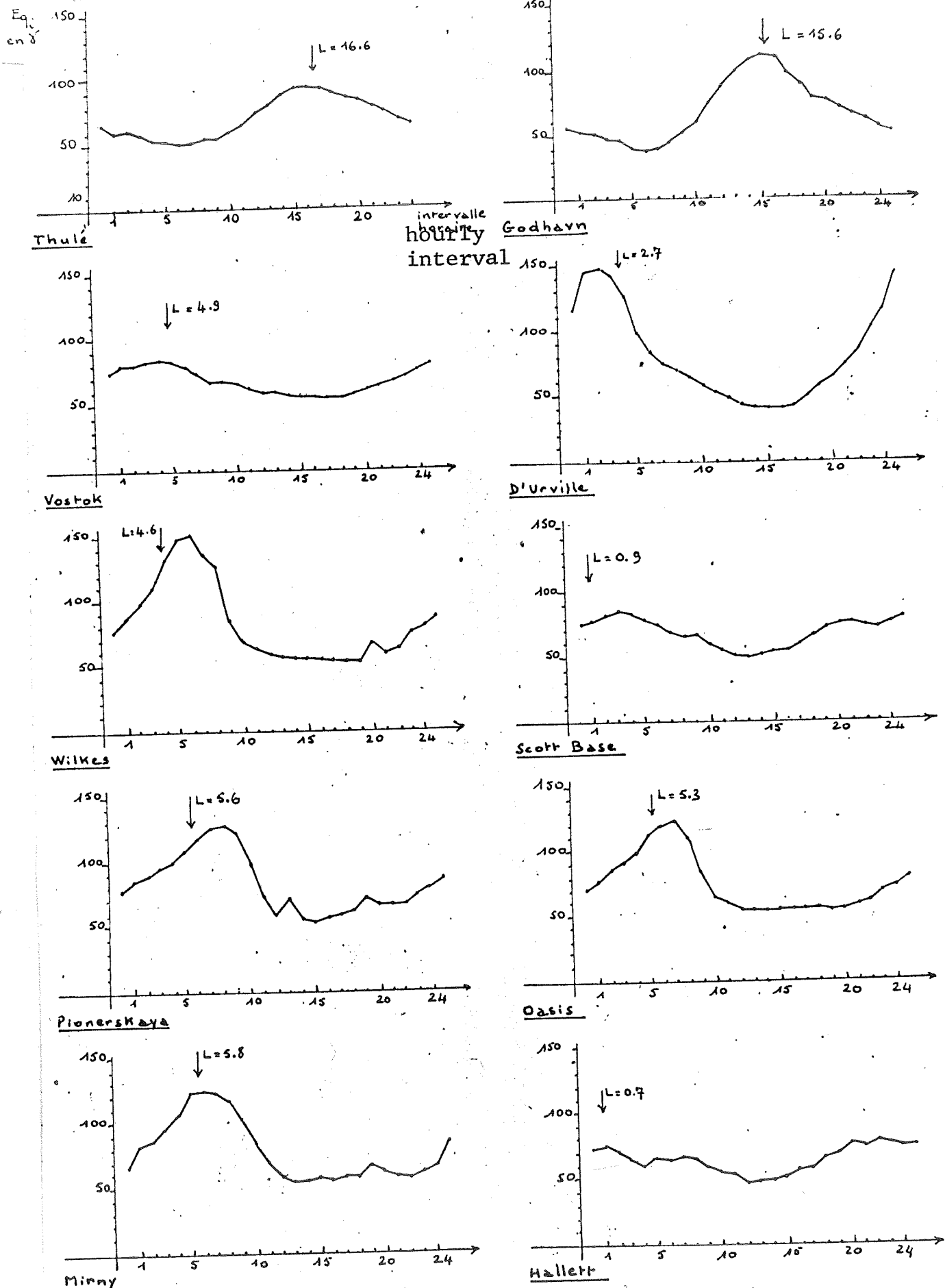


Fig. 6 Average daily variation of the E_{qi} dispersion of the current vector

Station	L heure du midi Local	H _a	i (minimum)
Vo	4.88	4.20	18
Du	2.67	1.60	16
Wk	4.64	5.31	18
SB	0.88	0.85	13
Po	5.63	6.40	15
Oa	5.29	5.20	19
Mi	5.80	5.40	16
Ht	0.65	0.20	12

Table 2 Values of the H_a hour of the maximum of the E_q dispersion and of the hourly interval i (minimum) for which the dispersion is minimal.

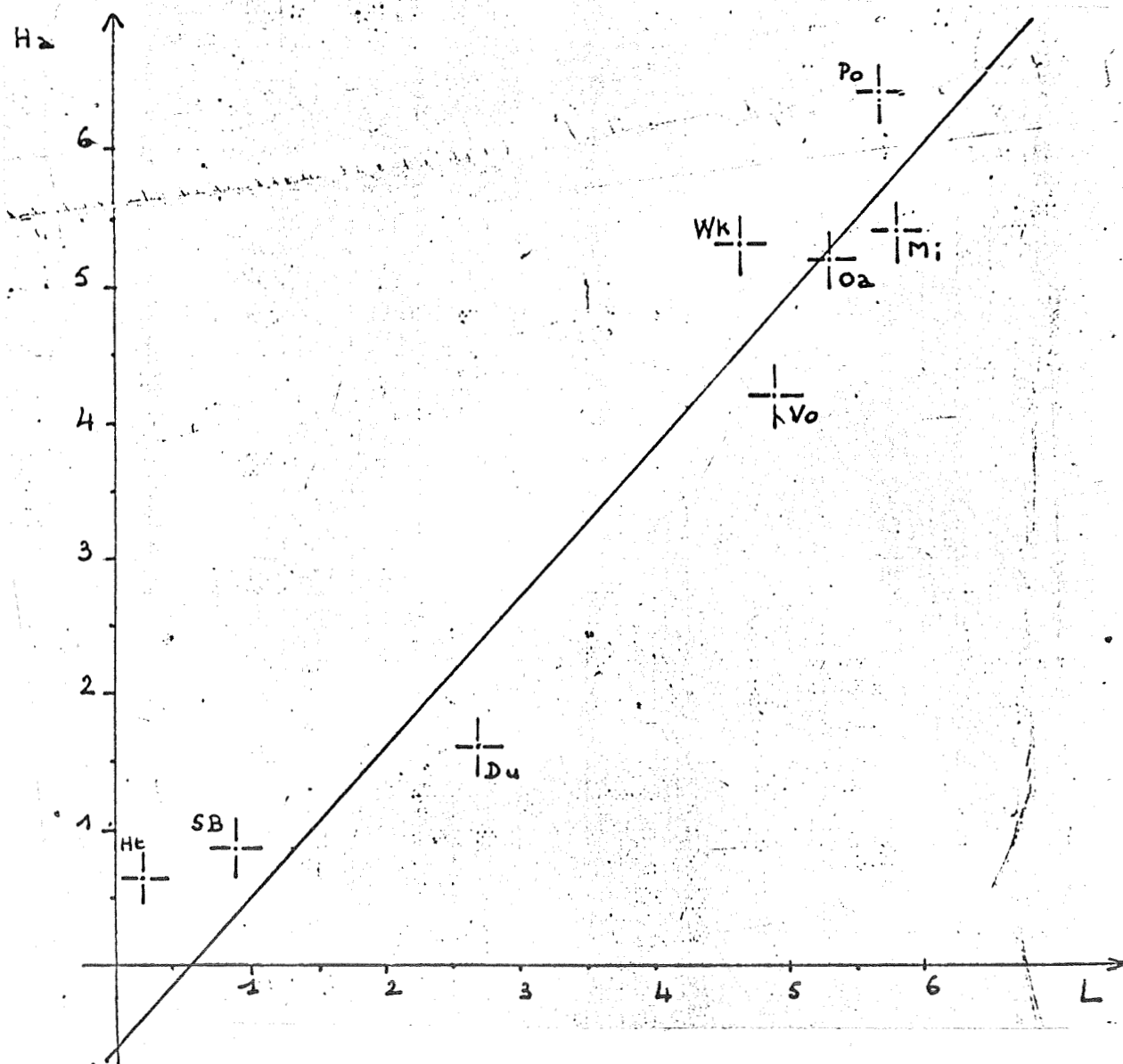


Fig. 7 Value of H_a as a function of L. The straight line of least squares was drawn.

1.2 Determination of calm days:

It is desirable to select days where the average density of the current is weakest; these are the days for which the I parameter is minimal.

Unfortunately, the calculations of I require in particular the knowledge of the zero of the current. This difficulty is alleviated by the fact that a great error in the calculation of zero has little effect on the value of I , and that a good correlation between the daily values of I and the corresponding values of the A_p planetary index exists. These two results were obtained by Lebeau (1965) for the Dumont D'Urville station. For other stations, the correlations between I and A_p , made evident in the work that follows, will bring about a justification a posteriori.

Calm days are defined as those days for which K_p is less than 10_0 . There were 31 calm days in 1958.

Having defined calm days and the calmest hourly intervals, X_{01} and Y_{01} whose values for the different stations are assembled in Table 4, will be determined with regard to the results obtained by the second method.

2. Hodograph method:

Hodograph of the horizontal component will be defined as the broken line that joins, in order, the 24 points P_i extremities of the \vec{H}_i vector. For a given station, hodographs relative to classes

of days of growing activity. The criterion of activity is the value of A_p . Note that it correlates well with the average daily intensity of I_j of the ionospheric current. Ten classes of approximately 70 days, which partially overlap and correspond to growing values of activity, were formed.

Class Classe	Value of A_p Valeur de A_p	Numbers of the 1st and last Numéros du premier et du dernier jour de chaque classe days of each class		No. of days Nombre de jours
1	2 à 6	1	71	71
2	5 à 7	29	91	62
3	7 à 10	72	148	76
4	9 à 12	110	179	69
5	11 à 15	149	214	65
6	13 à 18	180	245	65
7	16 à 23	215	279	64
8	19 à 31	246	314	68
9	23 à 48	275	340	65
10	27 à 200	296	365	69

Table 3

Figures 8.1 to 8.10 show the behavior of the hodograph of different stations in a function of the activity. As the activity decreases, the hodograph contracts regularly; it may be projected that at the limit, for a perfectly nul activity, the hodograph would be reduced to the P_0 point, which represents the undisturbed

-12²-

Fig. 8.1

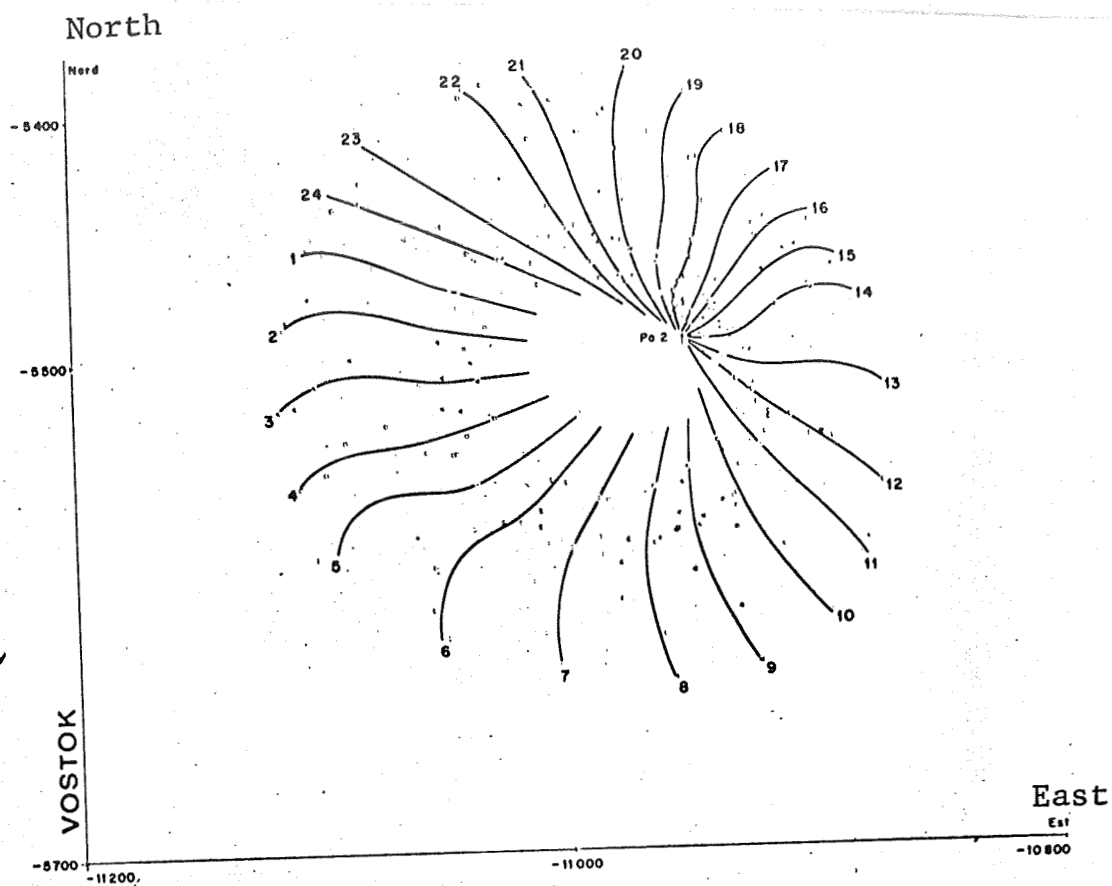
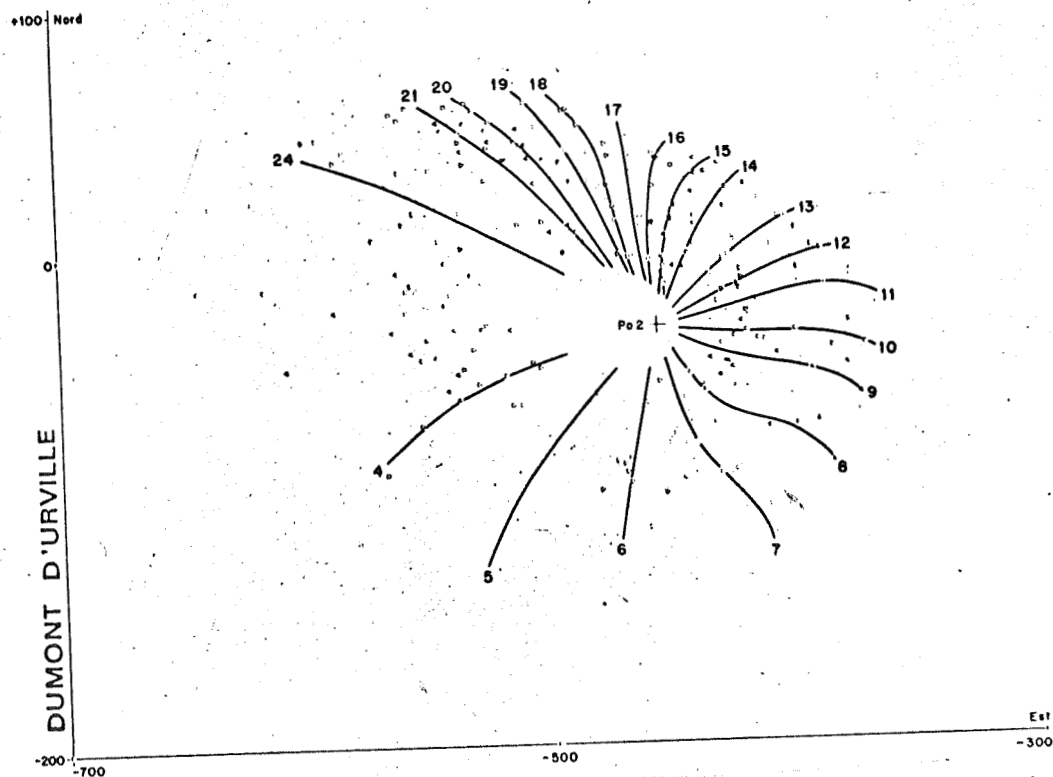


Fig. 8.2



Figures 8 Determination of the value of the undisturbed field by the hodograph method. The 10 points relative to the various levels of activity for an hourly interval are indicated by the same number

Po₂ is the convergence point of the curves

Po₁ corresponds to the calculation made by the first method.

Fig. 8.3

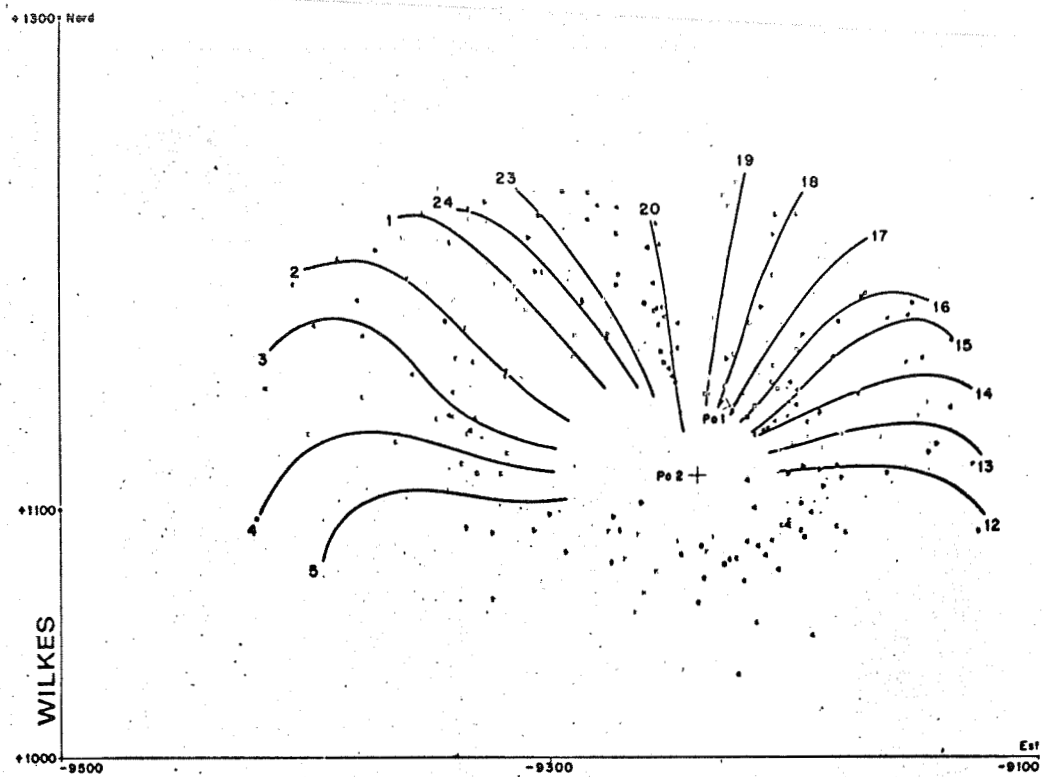


Fig. 8.4

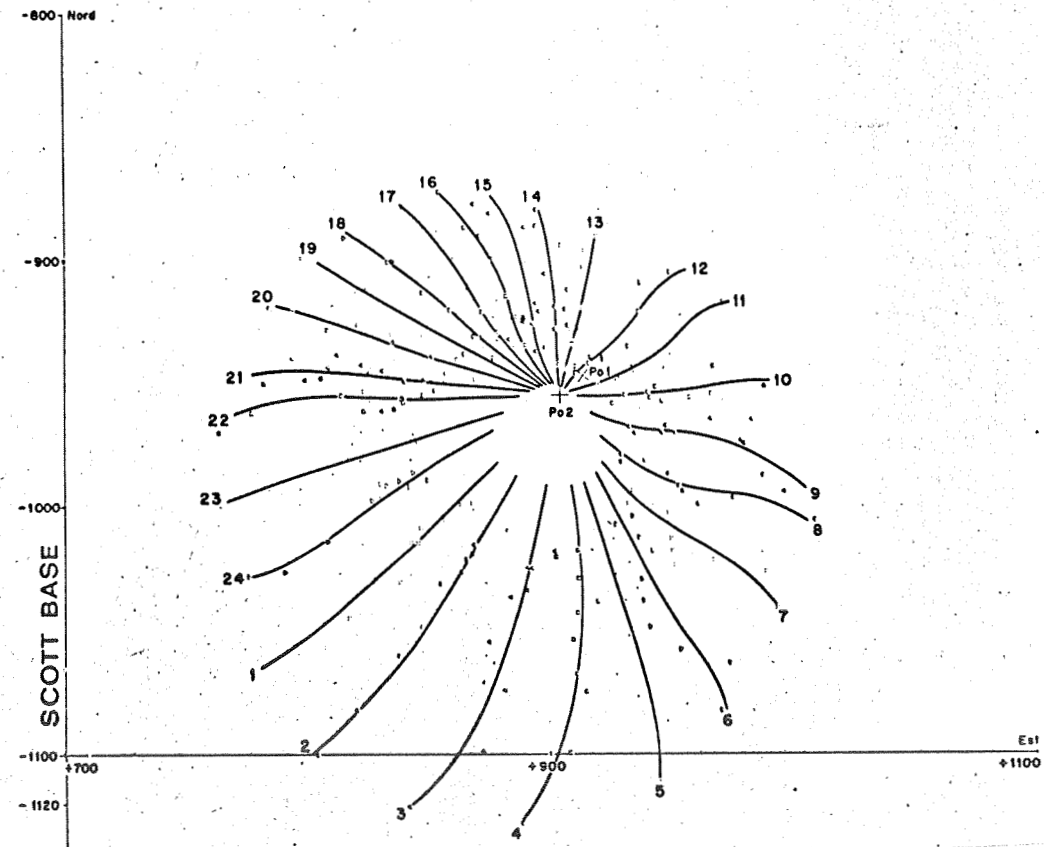


Fig. 8.5

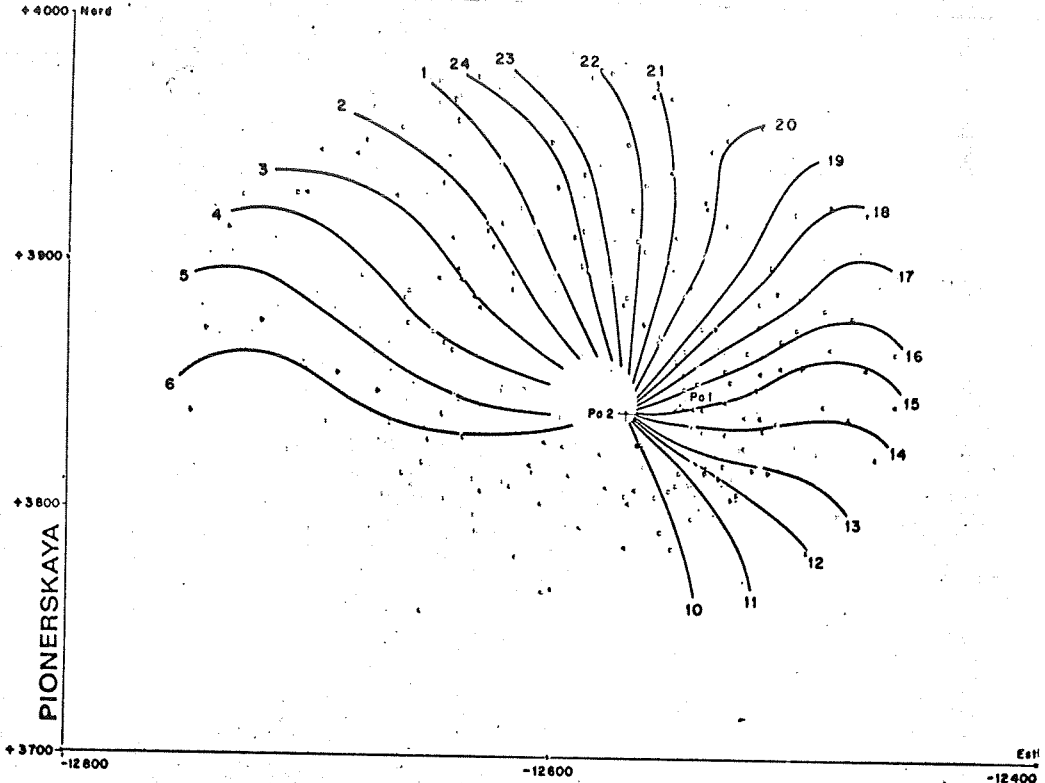


Fig. 8.6

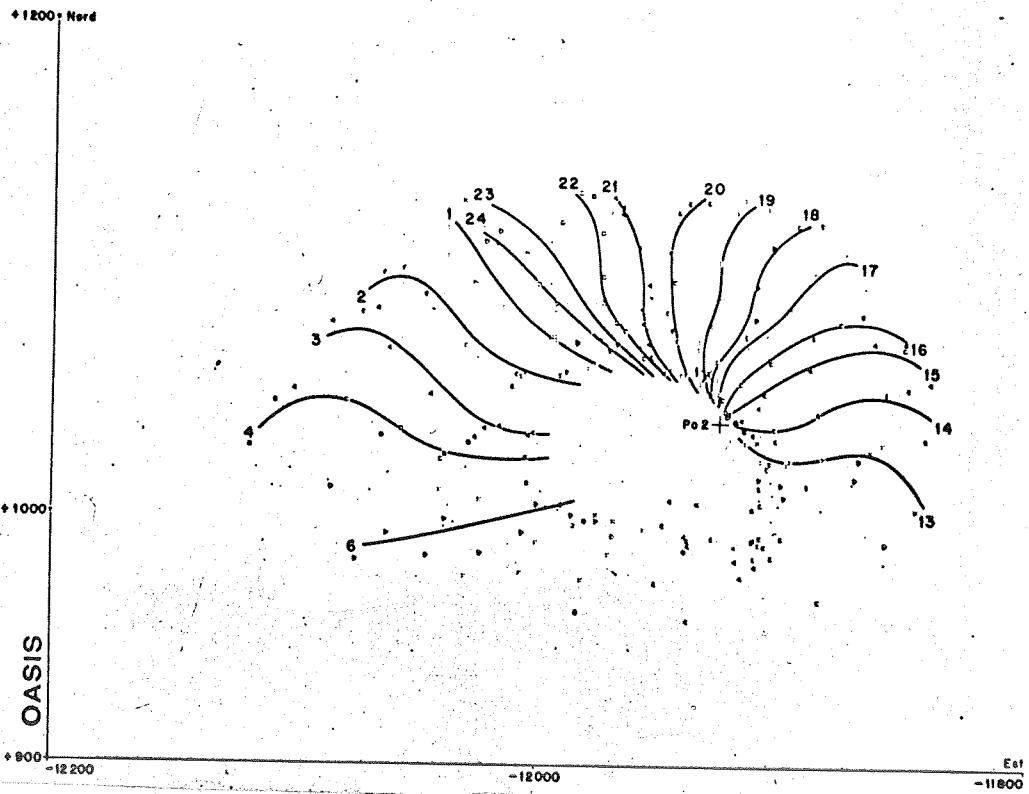


Fig. 8.7

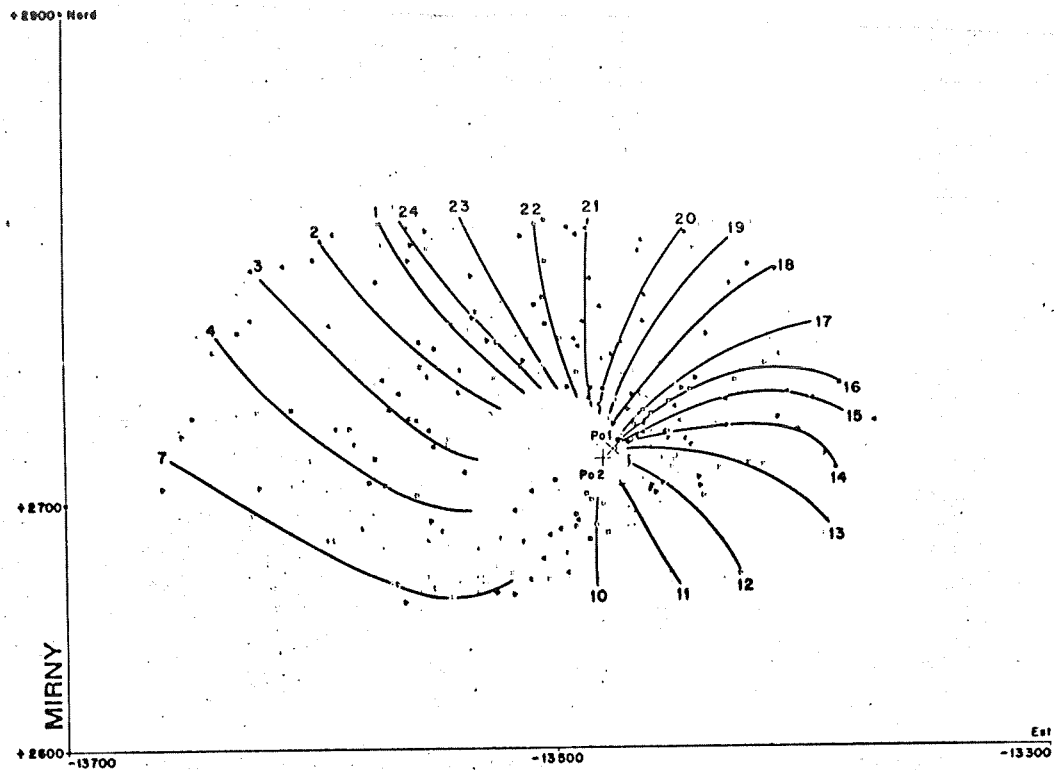
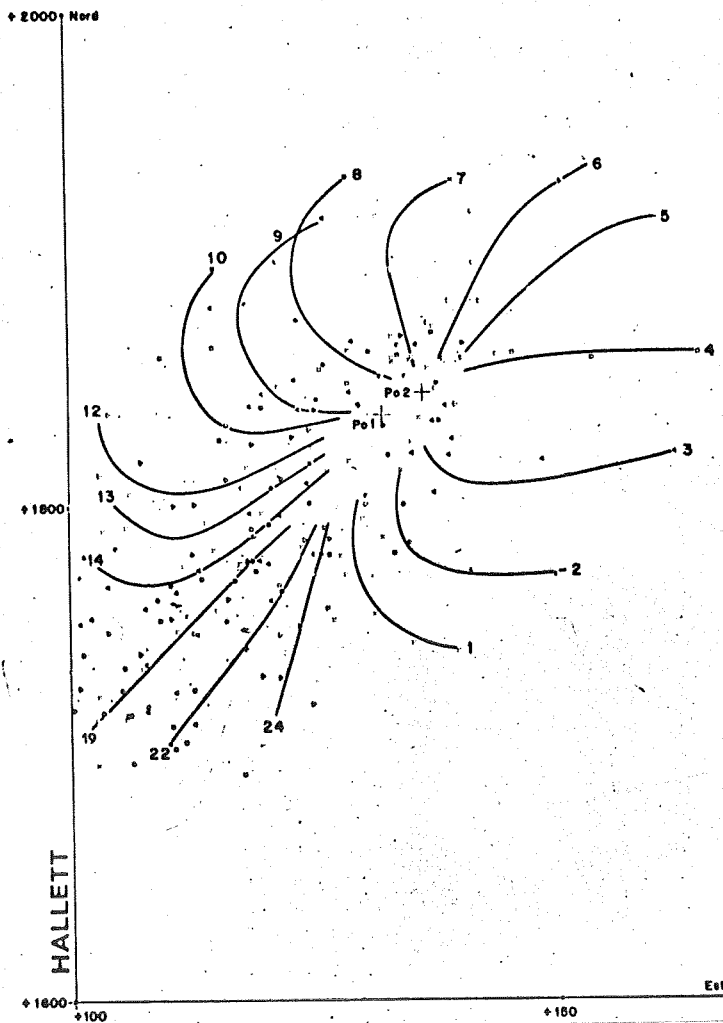
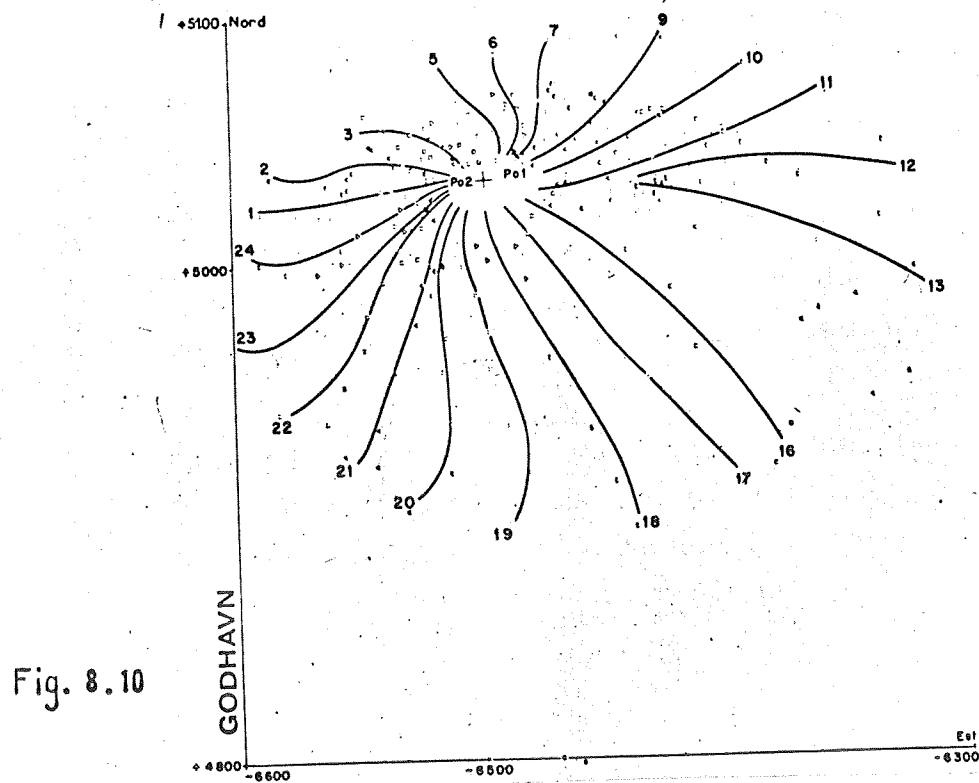
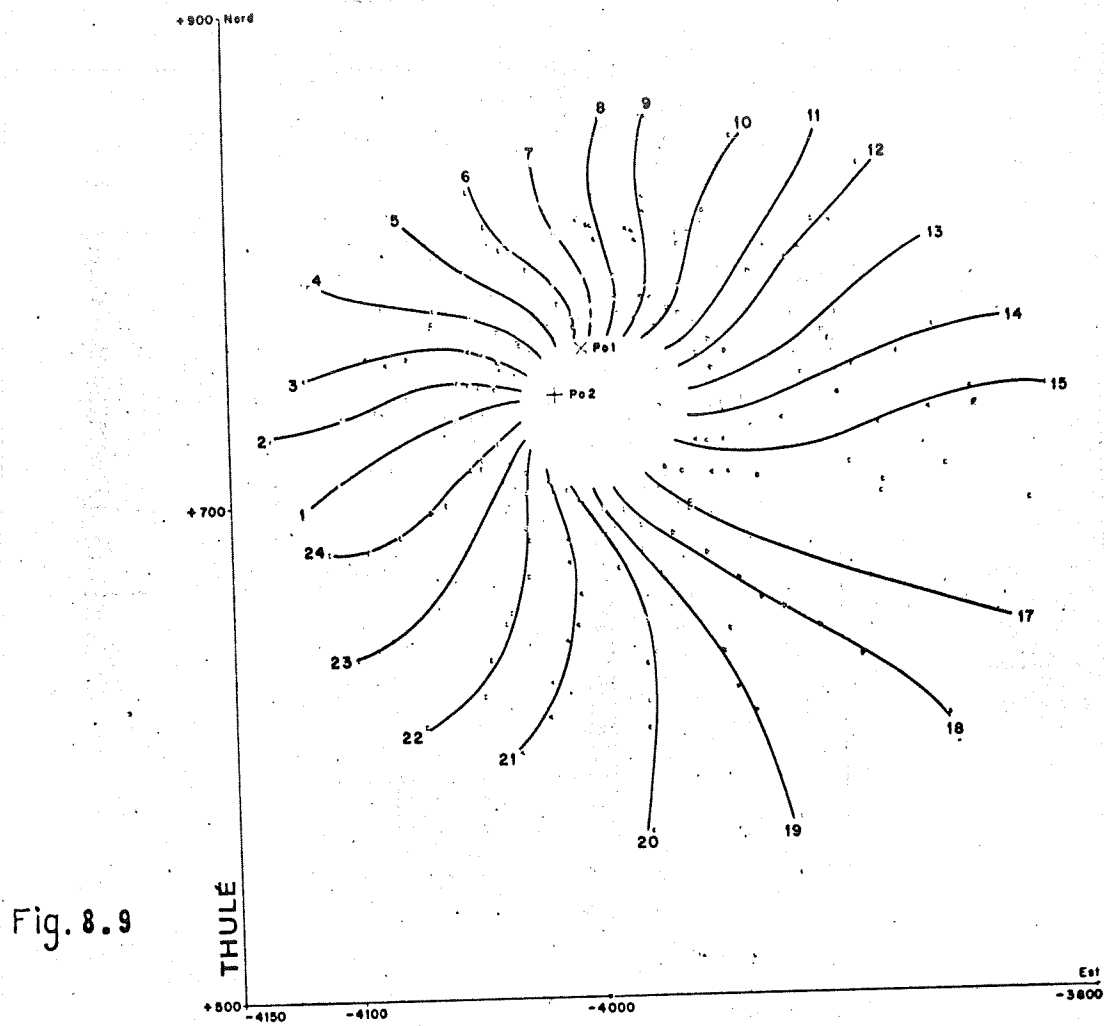


Fig. 8.8





field. Thus P_o will be determined by extrapolating the contraction of the hodograph; this is arrived at by drawing a curve that goes through the 10 points that correspond to the various levels of activity for each hour. At best, the point at which the 24 curves thus obtained for each hodograph converge can be estimated. Note P_{o_2} (X_{o_2} , Y_{o_2} , \vec{H}_{o_2}). Note that in all the cases studied, the uncertainty of the P_{o_2} position is less than 10γ ; some calculations made by different operators never vary more than 10γ .

The values of X_{o_2} and Y_{o_2} determined by this method are assembled in table 4.

3. Comparison of the two methods:

The value of the undisturbed field H_o will be defined as the value determined by the hodograph method:

$$\vec{H}_o \equiv \vec{H}_{o_2}$$

In fact the latter is affected by an uncertainty which seems less than 10γ whereas in the results obtained by the first method it is feared that a systematic error attached to the existence of a residual current exists.

The values of the difference between P_{o_1} and P_{o_2} are assembled in table 4; they show that the convergence between the two methods is excellent. Moreover, it can be considered that a fraction of this difference is due to a systematic error; the precision obtained on P_o is no doubt better than that which can be estimated from the

Station	X _{o1}	X _{o2}	Y _{o1}	Y _{o2}	P _{o1} P _{o2}
Vo	- 5 483	- 5 494	- 10 954	- 10 951	11.4
Du	- 12	- 31	- 453	- 455	19.1
Wk	+ 1 140	+ 1 113	- 9 226	- 9 239	29.9
SB	- 947	- 955	+ 913	+ 904	12.0
Po	+ 3 844	+ 3 840	- 12 548	- 12 570	22.4
Oa	+ 1 059	+ 1 039	- 11 930	- 11 926	20.4
Mi	+ 2 720	+ 2 717	- 13 476	- 13 480	5
Ht	+ 1 836	+ 1 846	+ 132	+ 136	10.8
Th	+ 761	+ 742	- 4 005	- 4 015	21.4
Go	+ 5 040	+ 5 032	- 6 480	- 6 495	17.0

Table 4

values of $\left| \overrightarrow{P_{o1} P_{o1}} \right|$. The point P_o will be assigned as the origin. The vector corresponding to an hourly interval given in taking P_o as the origin, and for the coordinates axes, the X axes toward the South, appears directly on the hodograph (fig. 9).

Fairchild (1962) in an analagous experiment used the the average value of the particular day for the value of the undisturbed

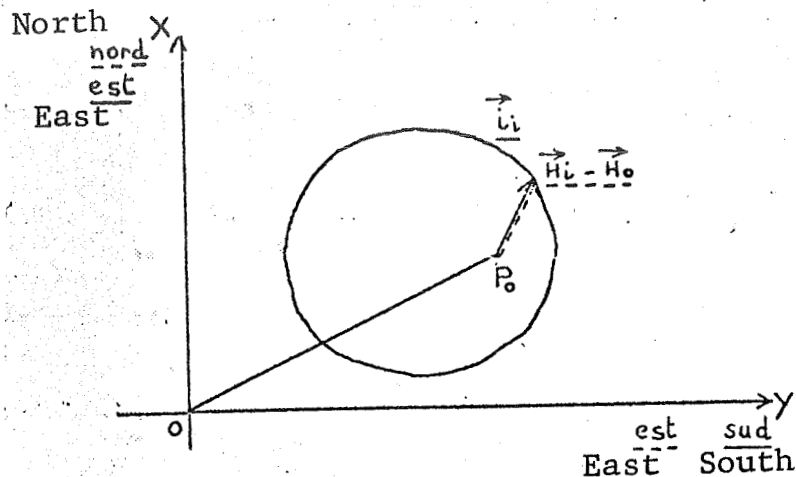


Fig. 9 The vectors \vec{i}_i and $\vec{H}_i - \vec{H}_0$ appear on the hodograph which must correspond to the axes: X, north and Y, east for the field vector, X east and Y south for the current vector.

field on a calm day, and for an agitated day, he took the average value of the field on a neighboring calm day. This method is highly subject to criticism. In fact, P_0 is generally not the barycenter of the P_i , even on a calm day. As an example, the position of the barycenter of the P_i on eight calm days in 1958 (four of which are cited in Fairfield's study) was determined. As seen in figure 10, they are at a distance of 12 to 60 γ from the point P_0 shifted systematically toward the zero in agitated times.

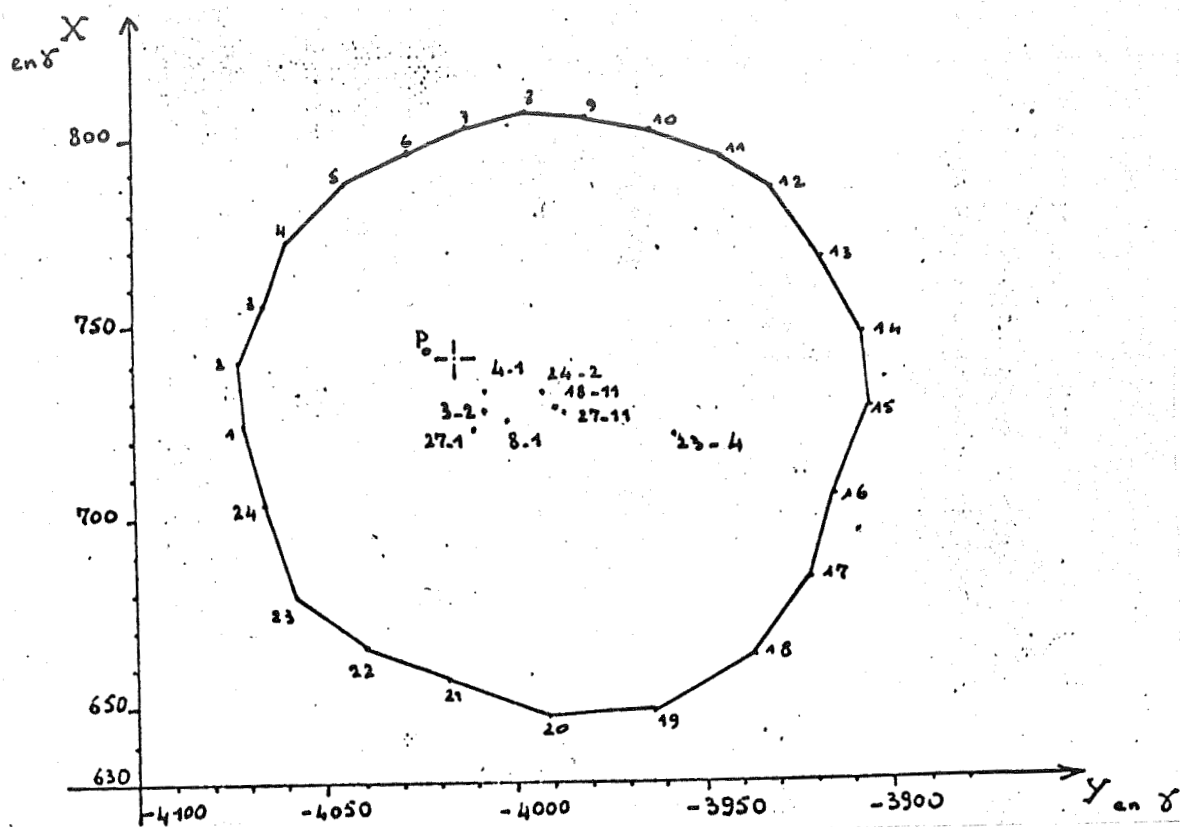


Fig. 10 Relative average hodograph at Thule. Comparison of the positions of P_o and of the origin points determined by the method of Fairfield for eight calm days. The variance is between 12 and 60 γ .

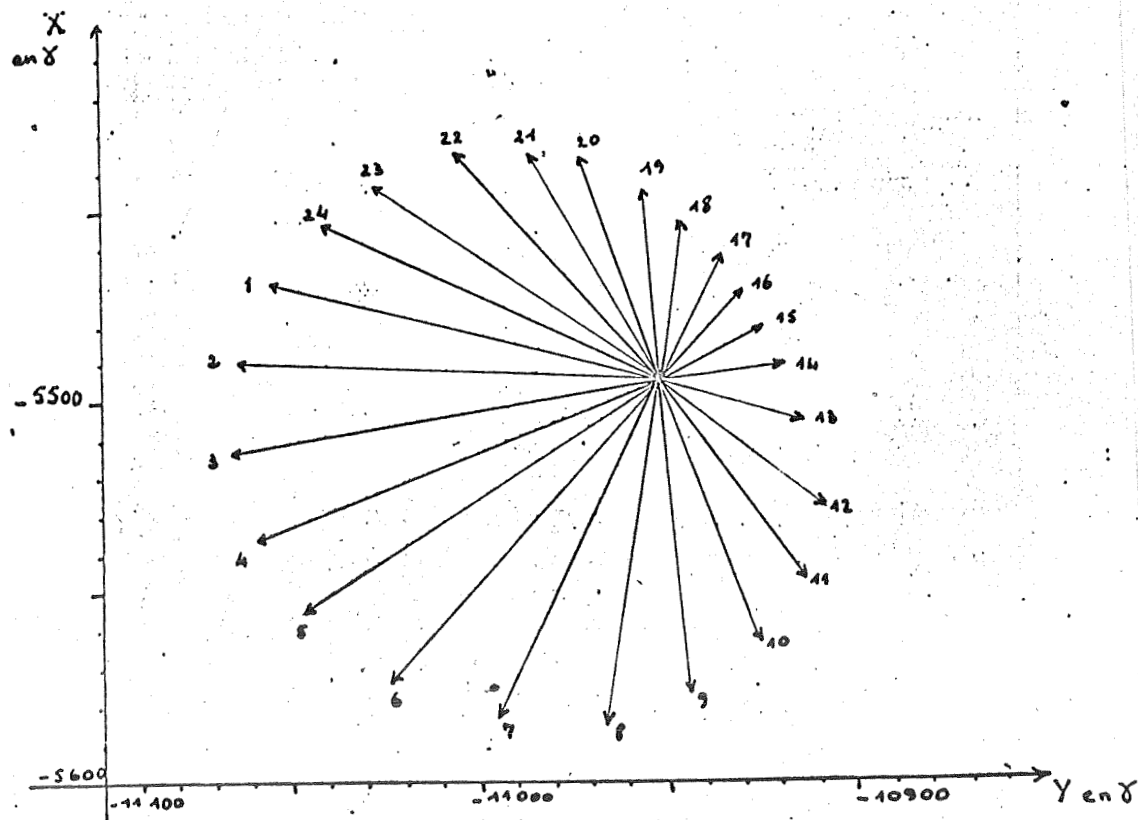


Fig. 12 Relative average hodograph at Vostok. Daily rotation of the current vector.

CHAPTER 3

Study of the Density of Current \vec{i} Vector

The study of the daily variation of the intensity and of the direction of the density of current \vec{i} vector will be undertaken.

The components of \vec{i} are immediately deducted from the components of \vec{H} , X and Y, whose values are recorded on digitaline tape for 15 stations over a 29 year period. The format of the recordings and the recapitulating table of the available data is described in annex 2.

1. The study of the intensity of the density of the \vec{i} current:

1.1. Calculation of the intensity:

The average annual intensity of i_i corresponding to the i^{th} hourly interval is the average of the intensities of the hourly vectors.

$$i_i = \frac{1}{n} \sum_{j=1}^n |\vec{i}_{ij}| \quad (n = 365 \text{ if no observation is missing})$$

The curve of variation of i_i as a function of the hour for each of the stations studied was drawn. The curves present a maximum in the vicinity of local noon (fig. 11.1 to 11.10). The hour of the maximum intensity H_{int} , is calculated as the abscissa of the highest point of the parabola passing through the highest point and through to points that surround it.

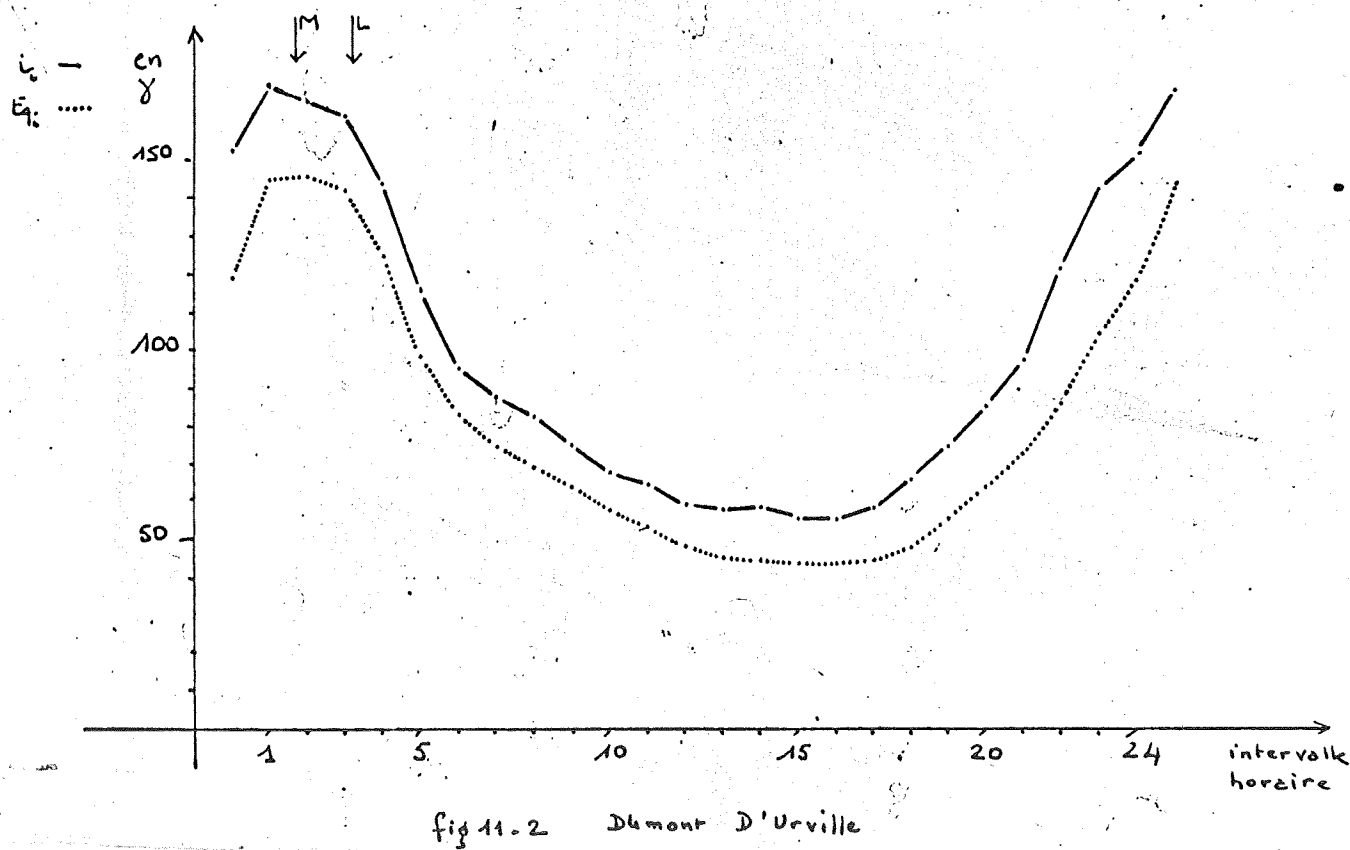
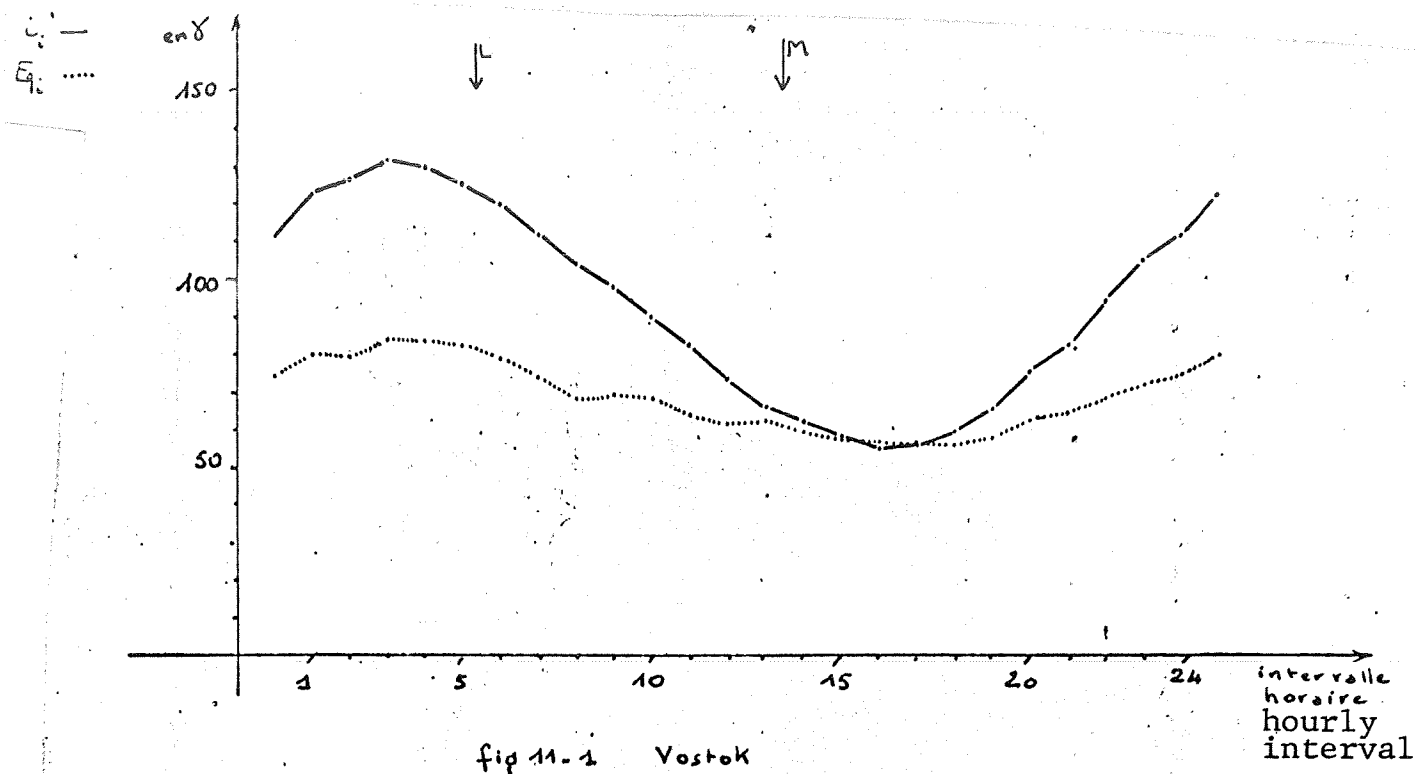
The effect of an error on the determination of the undisturbed field was evaluated by bringing the calculation in a parallel way from the origin P_0 , begins with the points P_E , P_N , P_W , P_S , distants from P_0 of $10r$ respectively in the east, north, west and south directions. The greatest shift ΔH_{int} of the hour of maximal results of one of these changes of origin is in all cases less than a half-hour.

Hallet station has peculiar properties, in spite of the fact that it has a magnetic colatitude of less than 14° . On one hand, the variation curve of the intensity as a function of the time presents two distinct maximums of comparable importance (fig. 11.8) On the other hand, the average hodograph has the appearance of an elongated oval, contrary to those of the other stations in the central regions of the polar caps, which are almost circular. It can be supposed that this local effect is related to the geographic position of Hallet, which is situated on the coast of the Antarctic continent at a point where the direction of this coast juts in sharply. This station will not be considered in the average results of the stations in the central region of the polar caps.

Table 5 contains the results relative to the stations studied.

1.2 Comparison of the daily variations of the intensities of the currents and of the magnetic activity:

The intensity of the density of the currents is maximal at an hour close to local noon.



Figures 11 Daily variation of the intensity of i_i of the density of the current. The curve of the daily variation of the dispersion was indicated by a pointed line Eq_i

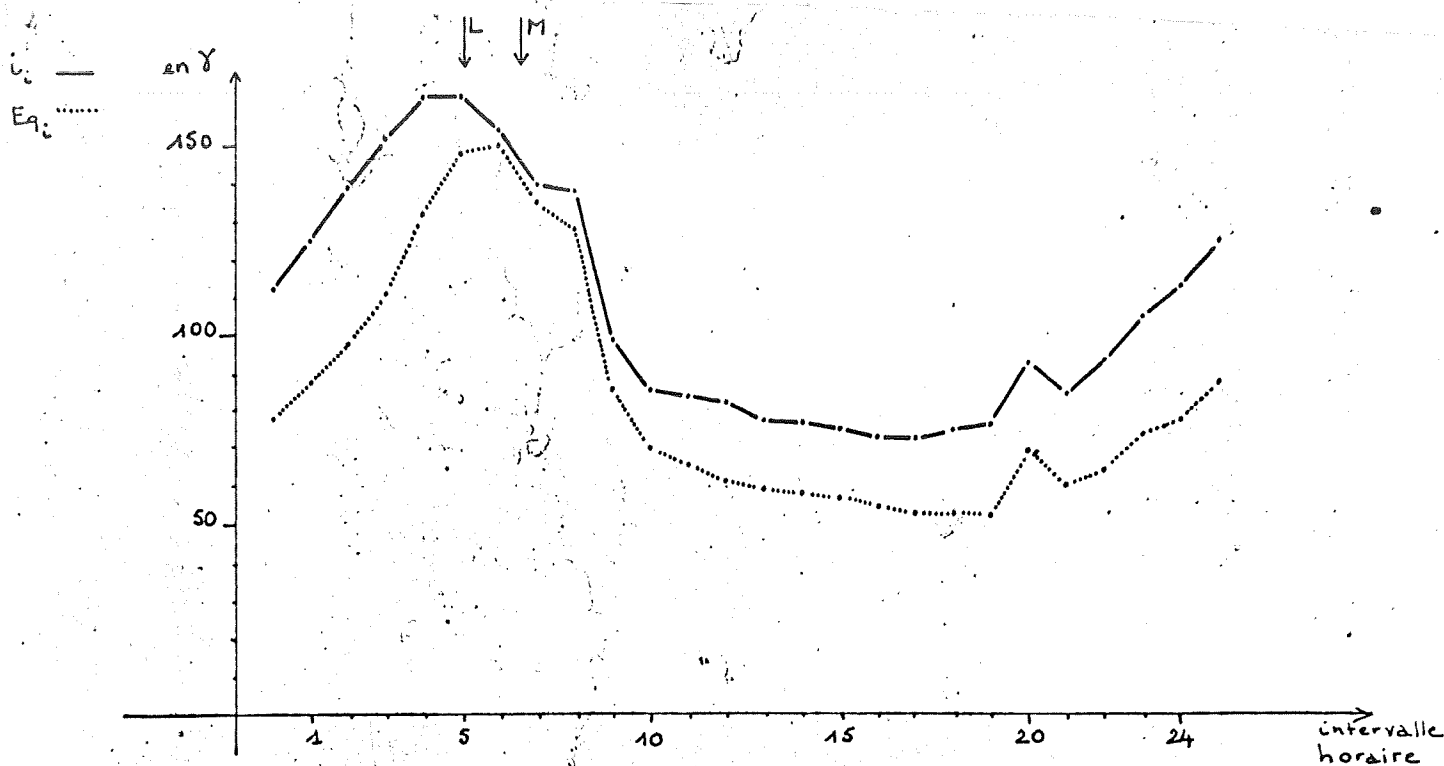


fig 11-3 Wilkes

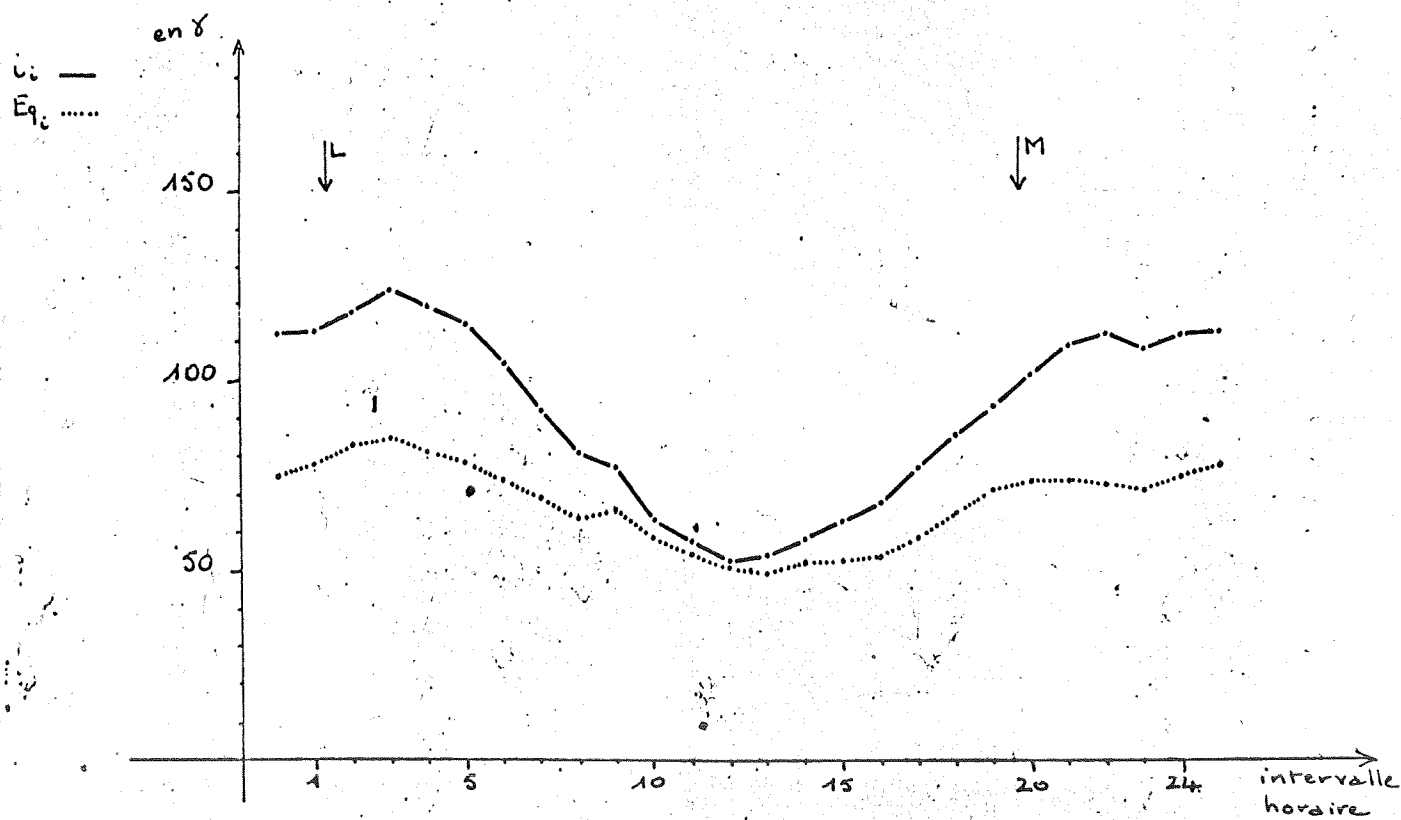


fig 11-4 Scott Base

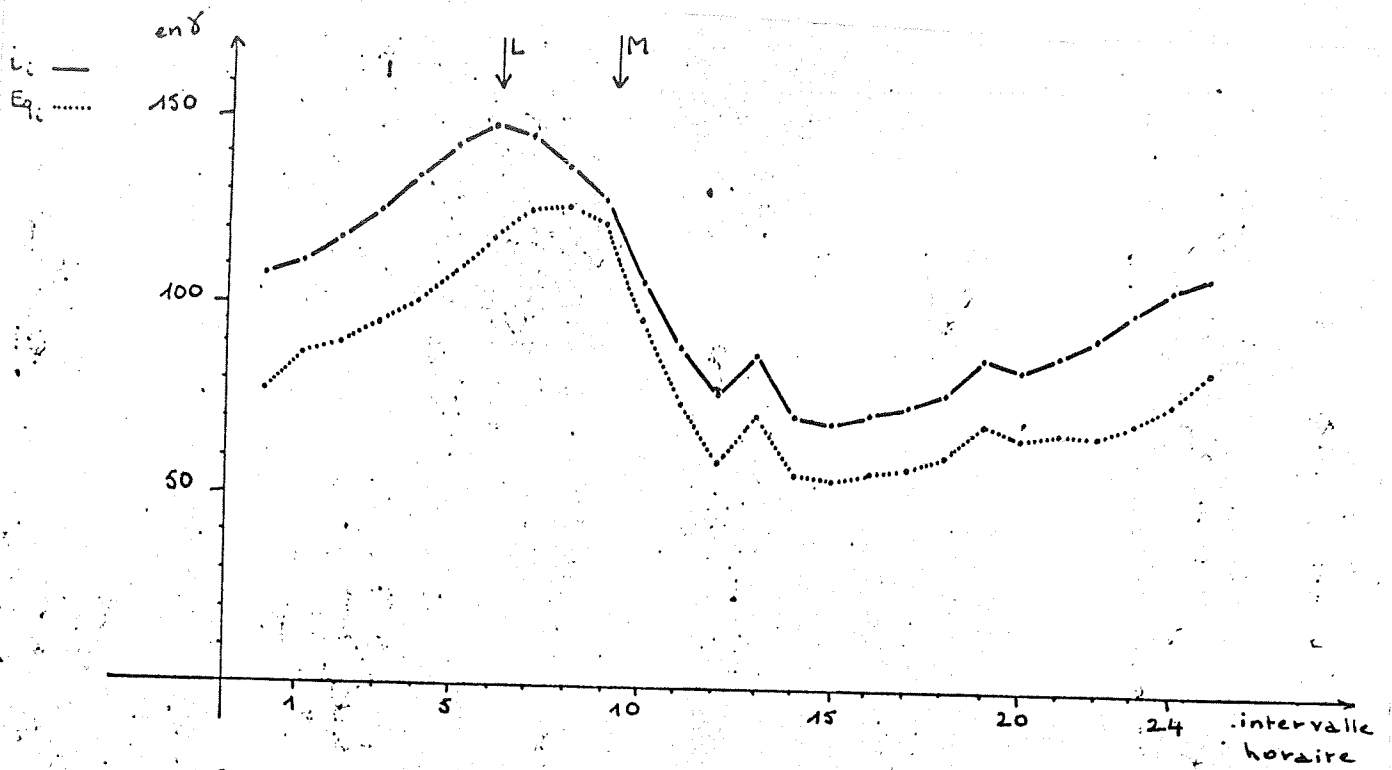


fig 11-5 Pionerskaya.

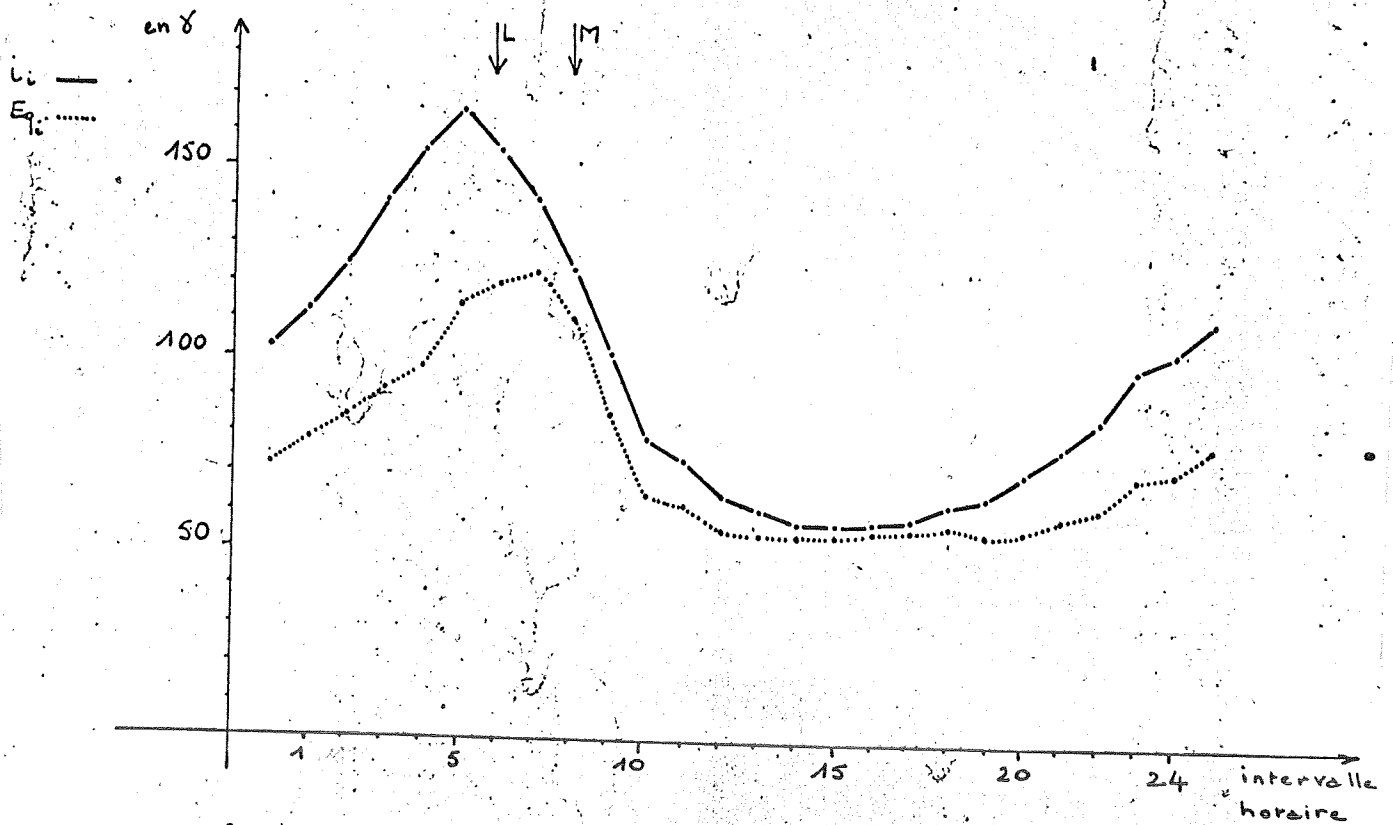


fig 11-6 Oasis

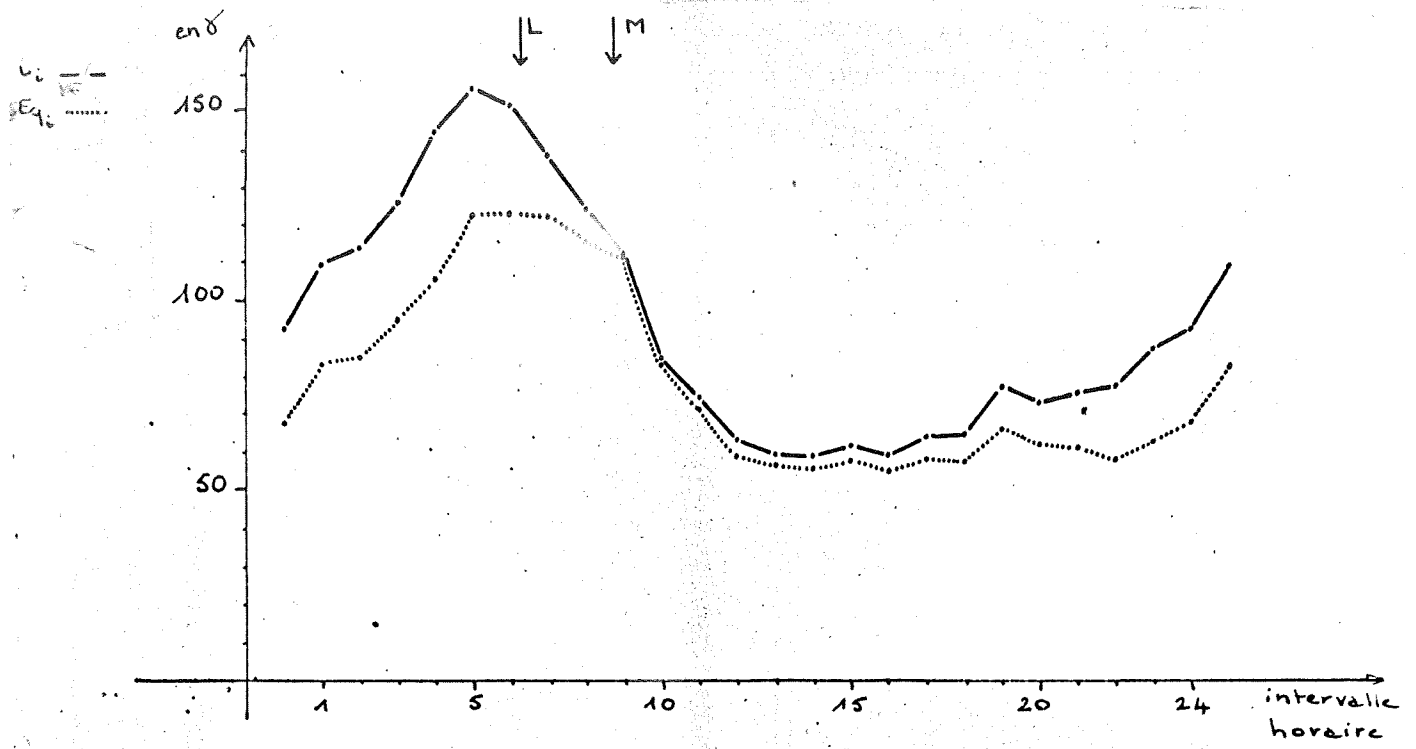


fig 11.7 Mirny

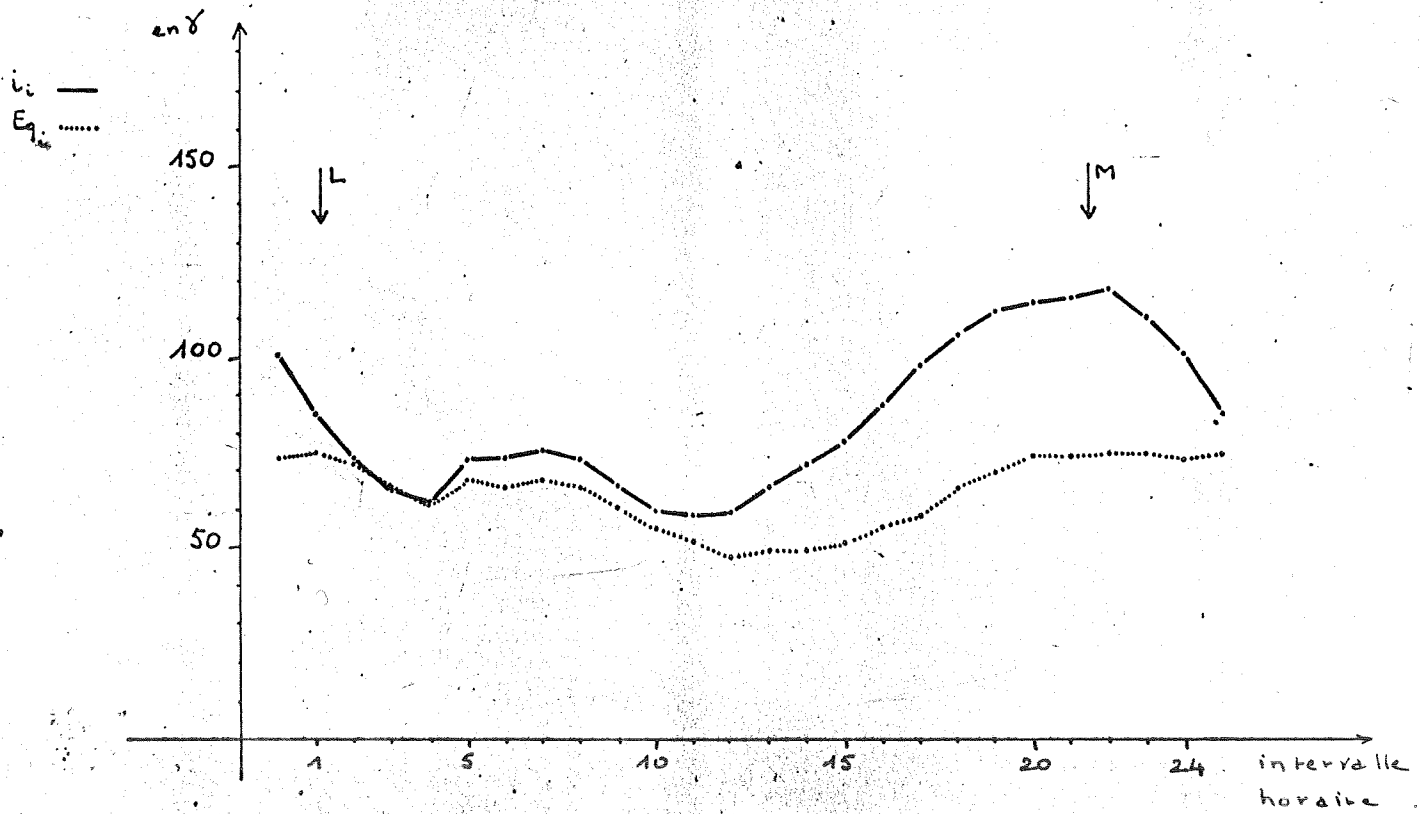


fig 11.8 Hallett

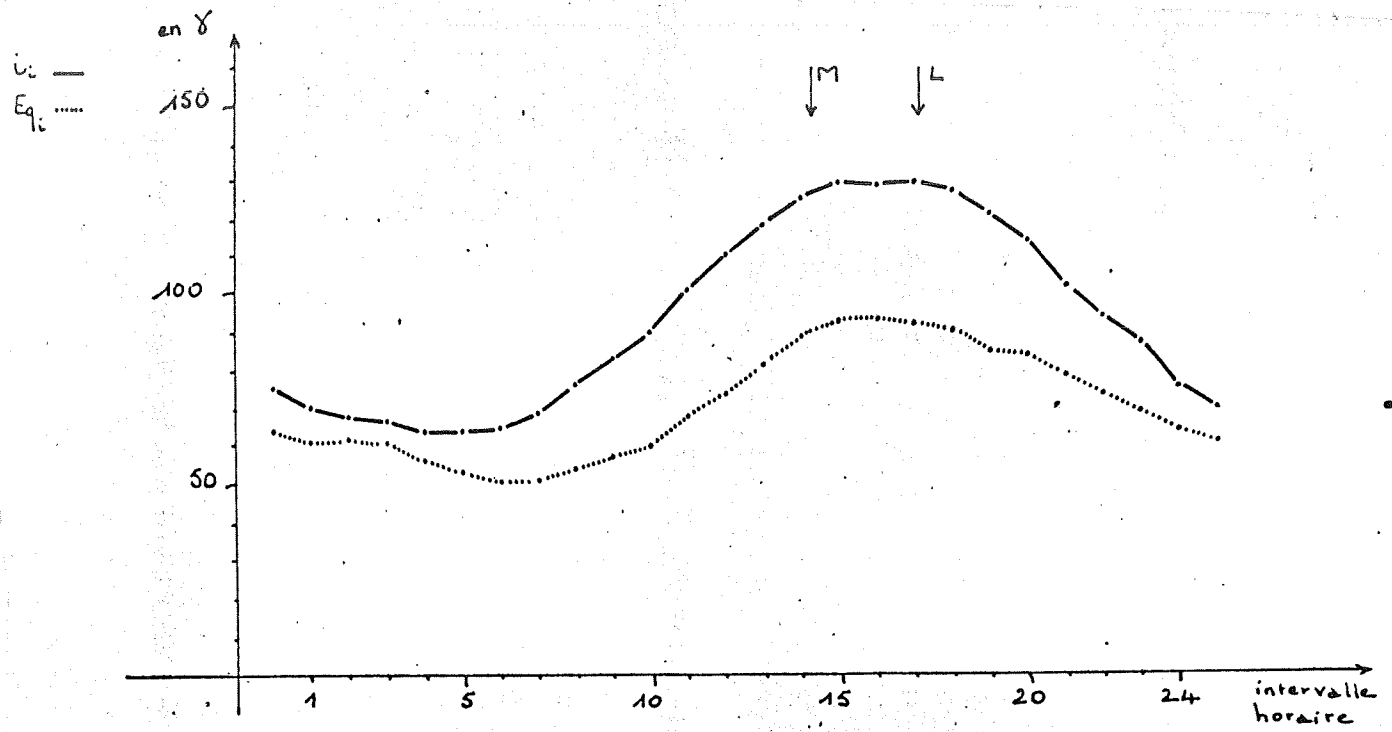


fig 11-9 Thulé

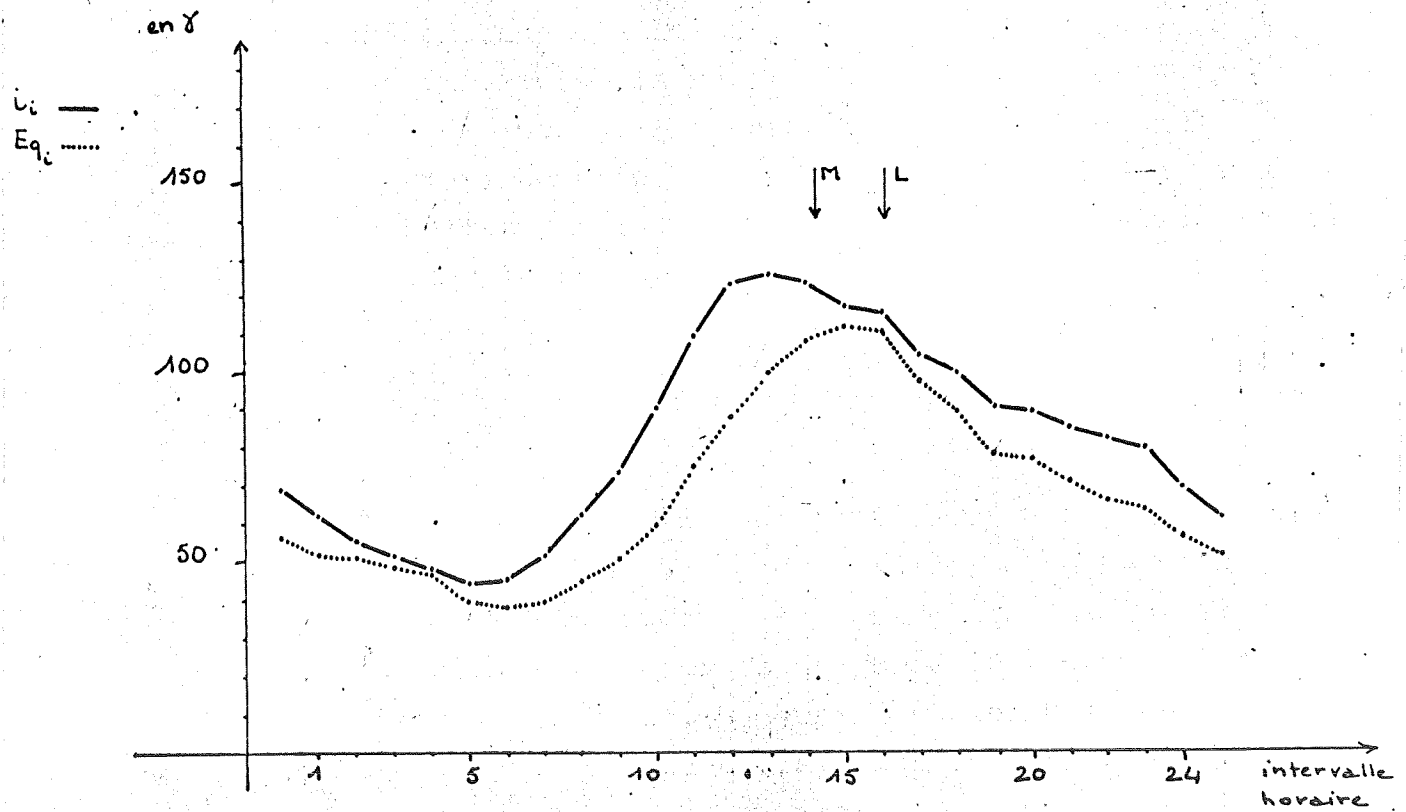


fig 11.10 Godhavn

Station	l_L	di local	H_{int}	$2\Delta H_{int}$ (pour un changement d'origine)	$H_{int} - L$
Vo	4.88		2.74	0.44	- 2.14
Du	2.67		0.83	0.07	- 1.84
WK	4.64		4.03	0.24	- 0.61
SB	0.88		2.57	0.20	+ 1.69
Po	5.63		5.76	0.25	+ 0.13
Oa	5.29		4.50	0.04	- 0.79
Mi	5.80		4.71	0.06	- 1.09
Th	16.61		16.58	0.02	- 0.03
Go	15.57		12.52	0.15	- 3.05

Legend

1-Local noon

$2-\Delta H_{int}$
(for a change in origin)

Table 5 Value of the hour of maximum current intensity

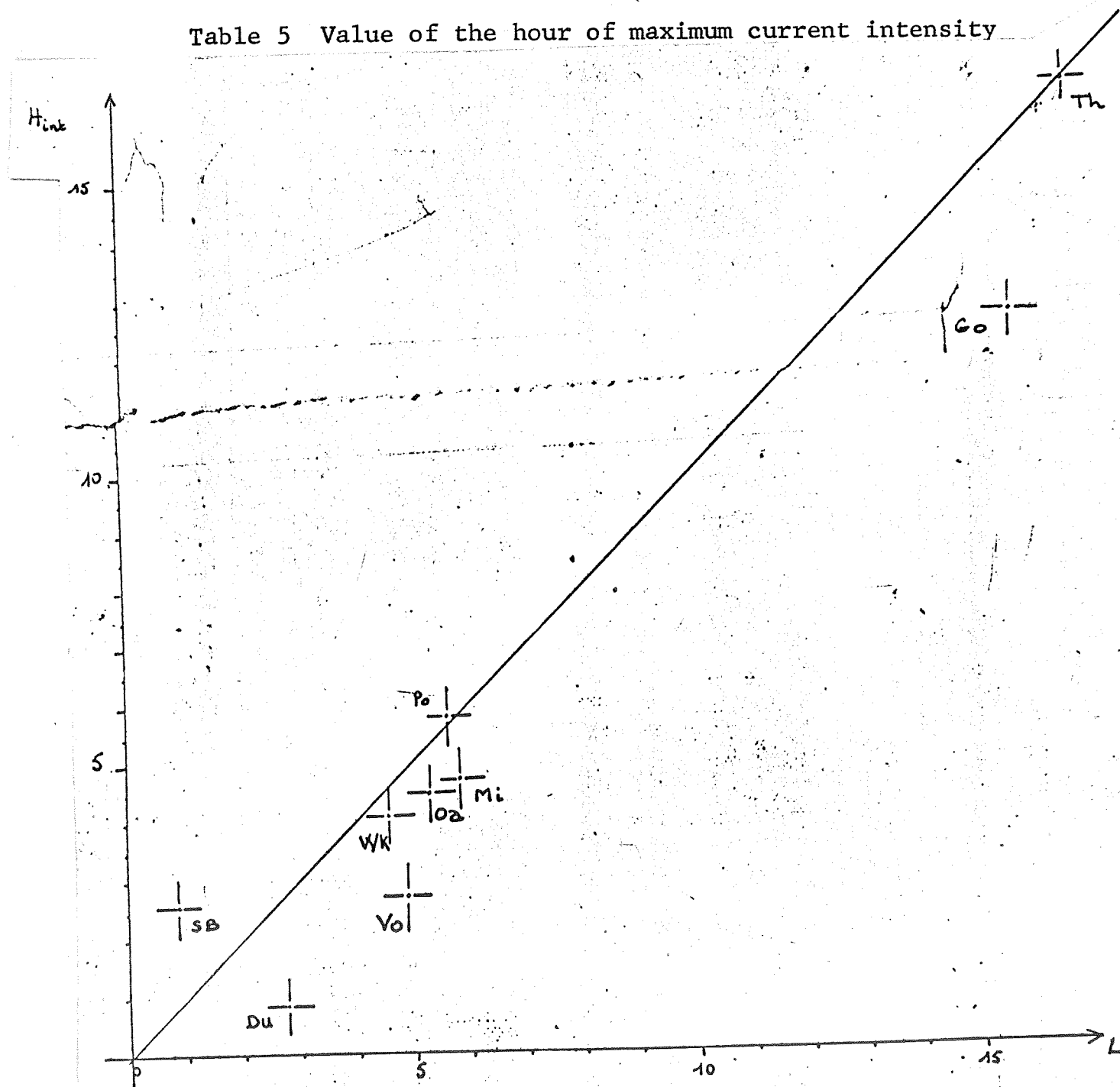


Fig. 13 Value of the hour of maximum intensity H_{int} compared to the hour L of local noon. A straight line was drawn $H_{int} = L$

The difference $H_{int} - L$ is superior to the shift corresponding to the uncertainty of origin. Its average value in modulus is 1.26 h. Its relative average value is - 0.86 hour. The H_{int} value is shown as a function of L in figure 13.

The divergence observed is not systematically directed towards the magnetic noon. Notice, however, on the curves relative to certain stations (Du, Wk, SB, Po, Th, Go, figures 11 -2, -3, -4, -5, -9, -10) the presence of a secondary maximum near the M hour.

It is known that the daily variation of the magnetic activity is characterized by a maximum at hour H equidistant between local noon L and magnetic noon M. The results thus obtained vary greatly from this behavior. If the explanation proposed by Lebeau (1965) to interpret the behavior of the activity described by the K indexes: action combined with a modulator mechanism, the variation of the conductivity of the E region, which tends to produce a maximum at local noon, and with an excitator mechanism which reacts with the maximum intensity at the hour of magnetic noon, it must be admitted that the effect of the modulator mechanism is heavy in the daily behavior of $|i|$.

1.3. Justification of the hypotheses " E_{qi} varies with i_i ":

The first method of determining the origin was based on the idea that the dispersion of E_{qi} of the field vector and the average intensity i_i were minimal at the same time. The comparison of the

daily variation curves of E_{q_i} and i_i (figures 11.1 to 11.10) justifies largely this hypothesis and brings a remarkable correlation right between these quantities into evidence.

2. Study of the direction of the density vector of the current:

The average current vector appears directly on the hodograph beginning with the origin of P_0 . Its direction varies as a function of the hour in a nearly uniform way (fig. 12, p. 15²); it seems to approach the direction of the sun, to which it has already been systematically compared. The rotation of the vectors studied has been represented in a diagram in which the hour was assigned to the abscissa and the direction of the vector to the ordinate, counted positively toward the west. The daily uniform rotation towards the west will be represented by a straight line of the slope $+ 15^\circ/\text{hour}$.

2.1. Azimuth of the sun:

The daily variation of the azimuth of the sun depends on the time of year and on the latitude of the station; this is not true at the poles, however, where in all seasons the azimuth of the sun varies uniformly by 360° in 24 hours.

For the stations studied which were stations in the higher latitudes it can still be considered that the daily variation is linear, in the first approximation.

Fig. 14 represents the exact azimuth of the sun as a function

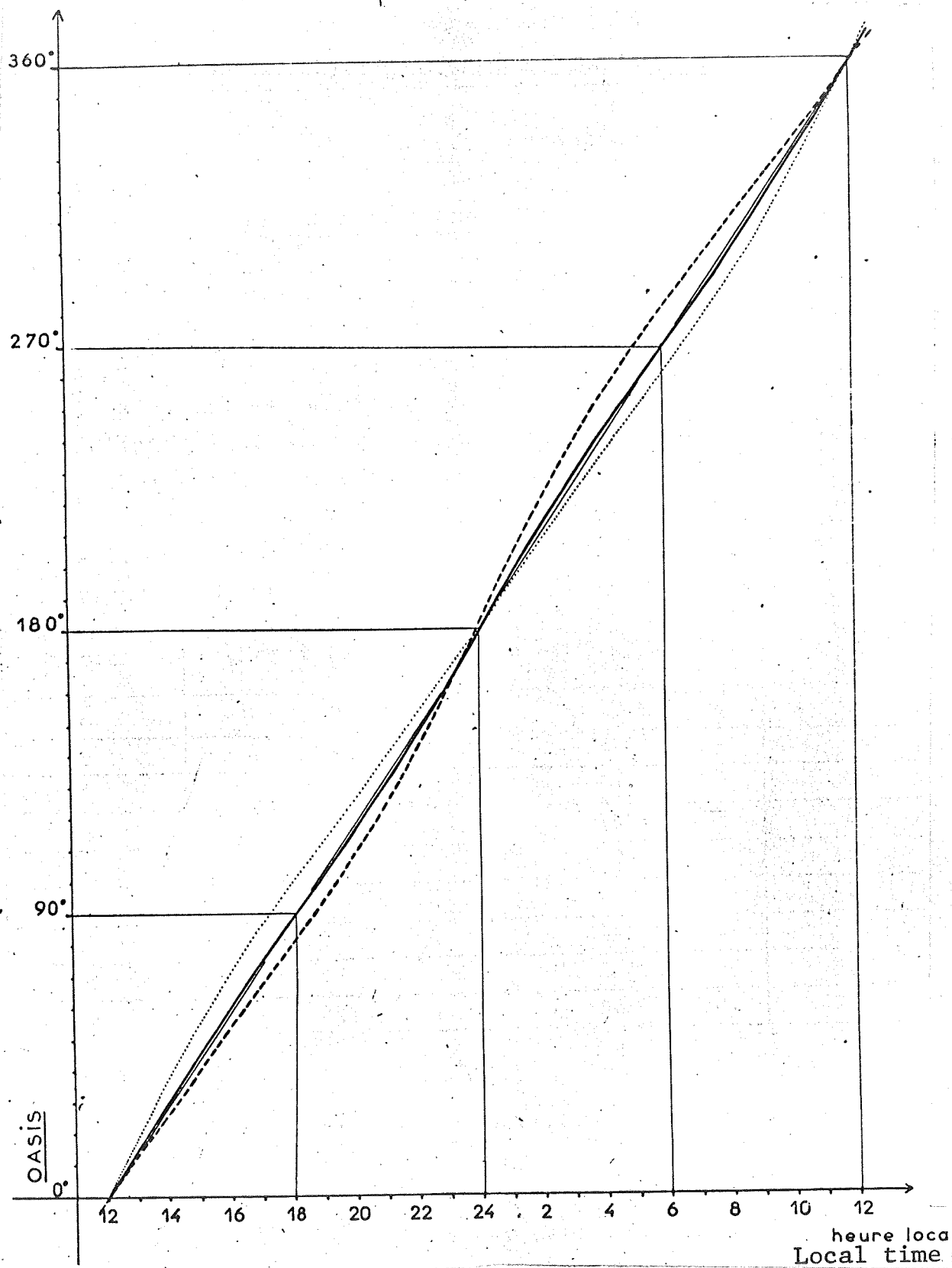


Fig. 14 Exact values of the azimuth of the sun at Oasis at the equinox (solid line), at the solstice of June (dotted line) and at the solstice of December (dashes).

of the hour for the equinox and the solstices at the Oasis station, which is the lowest in geographic latitude of all the stations studied ($=66^{\circ}16'$). The corresponding curves never vary more than 12° from the straight line which corresponds to an approximation of a uniform rotation.

2.2 Direction of the current vector averaged over a period of one year.

The direction of the current vector shifts systematically toward the west as compared to the azimuth of the sun; this is true for the Arctic stations as well as for the Antarctic stations (fig. 15.1 and 15.2). The daily variation of the direction of the current is not quite linear, nor is the variance observed between the direction of the current and the azimuth of the sun constant. A maximum occurs at an hour bordering on an hour of minimal intensity and a minimum corresponds to a maximum of intensity. In figures 15.1 and 15.2 the value of the intensity $|\vec{i}_i|$ was diagramed perpendicular to the straight line of the variation of the azimuth of the sun for each hourly interval. The values of the maximum and the minimum variances relative to the stations studied are assembled in table 6 (p. 21).

2.3. Effect associated with the magnetic activity:

The daily variations of the direction of the average current was compared on two classes of days. One corresponds to a weak

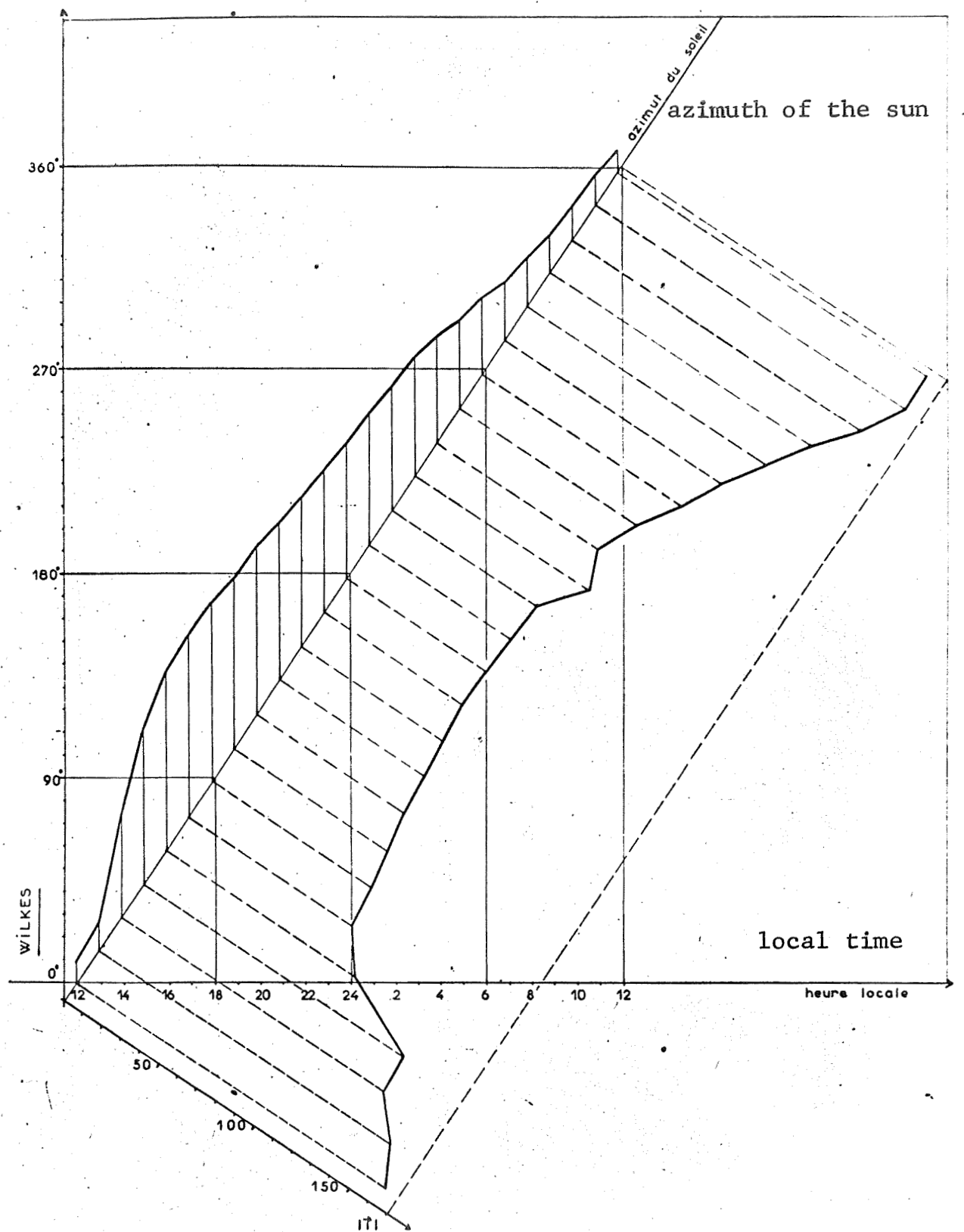


Fig. 15.1 Daily variation of the direction of the average current vector at Wilkes. The variance between this direction and the azimuth of the sun is compared to the average intensity of the current vector.

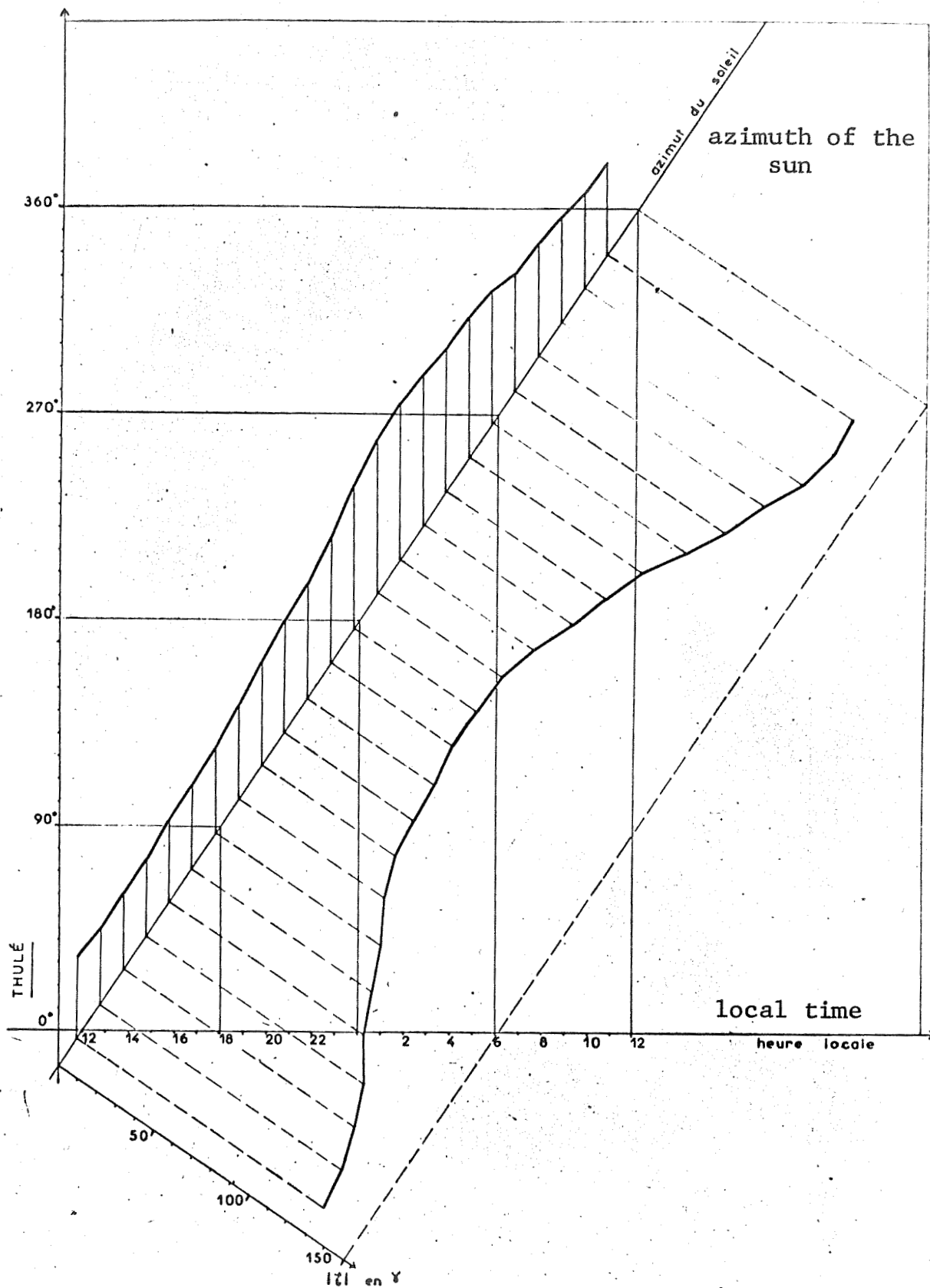


Fig. 15.2 Daily variation of the direction of the average current vector at Thule. The variance between this direction and the azimuth of the sun is compared to the average intensity of the current vector.

Station	Ecart Minimum Minimum variance	Ecart Maximum Maximum variance	Différence
Vo	37°	71°	34°
Du	9°	77°	68°
Wk	10°	79°	69°
SB	46°	85°	39°
Po	3°	60°	57°
Oa	20°	73°	53°
Mi	2°	74°	72°
Th	28°	59°	31°
Go	26°	86°	60°

Table 6

magnetic activity and to a weak average current, and the other corresponds to a strong magnetic activity. These curves (drawn for Vostok and Thule, figures 16.1 and 16.2) are rather close to the hour of maximum intensity, but at the hour of minimum intensity, the curve relative to the class of weak activity increases its distance from the direction of the sun.

2.4. Effect of an error of origin:

It might be asked if the lack of regularity in the rotation of the current vector may not be the effect of an error in determining the undisturbed field. The fact that the variance is maximum for the weakest values of $|i|$ would lead to that conclusion. To avoid this difficulty the effect of an error on P_0 was systematically studied.

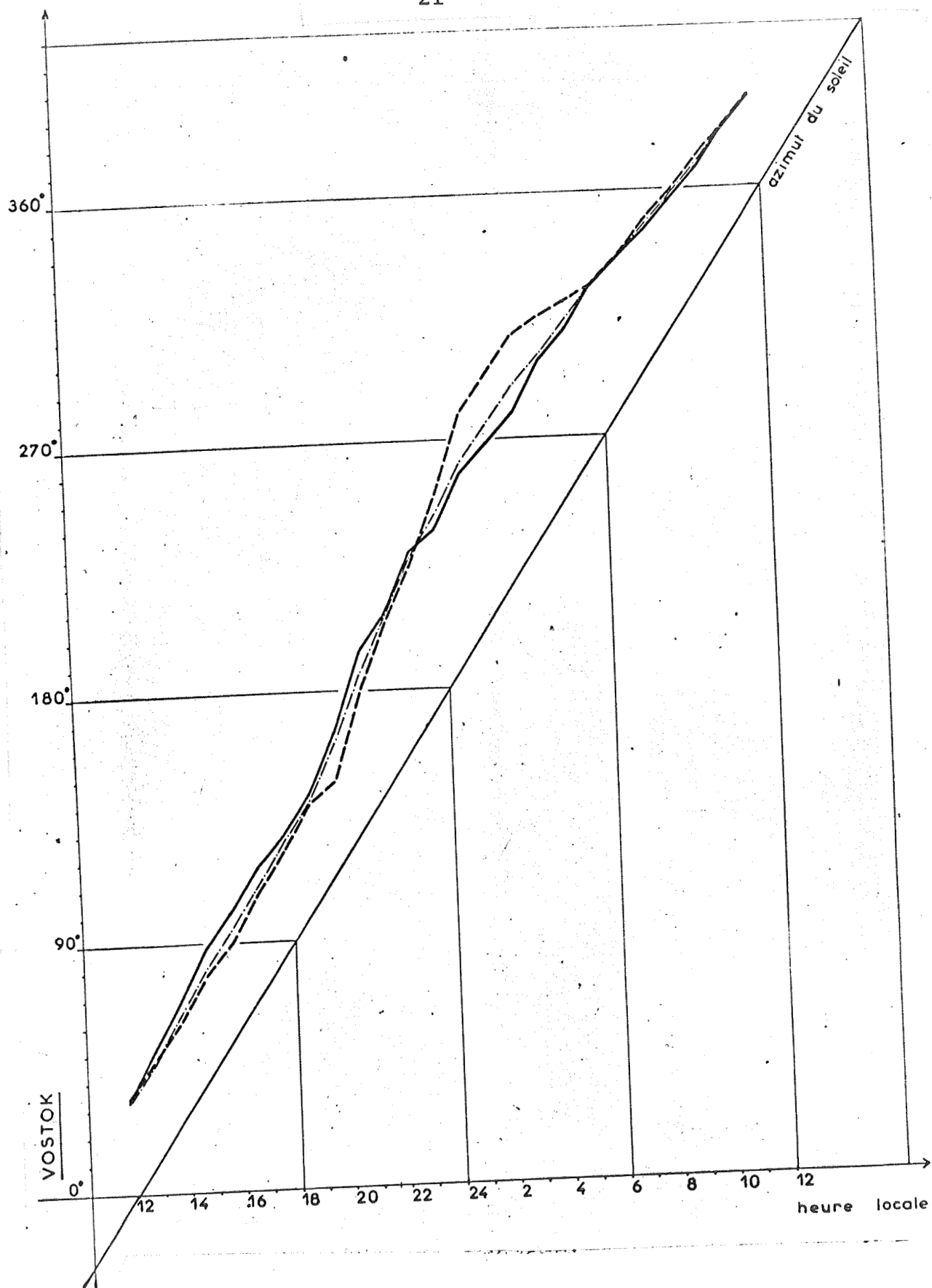


Fig. 16.1 Daily variation of the average current vector at Vostok for the classes of days of strong magnetic activity (solid line), of weak magnetic activity (dashes) and of average magnetic activity (dots-dashes)

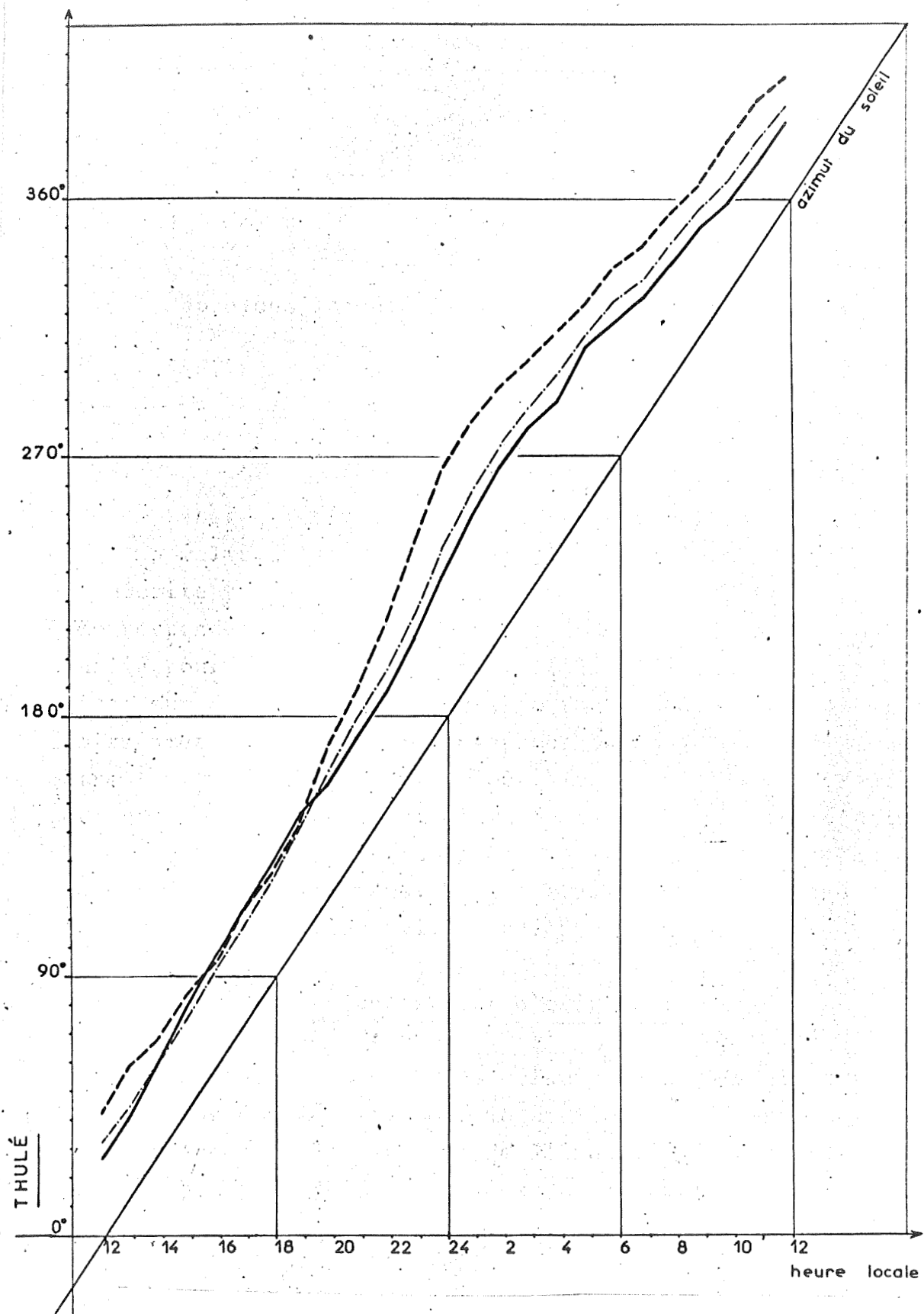


Fig. 16.2 Daily variation of the average current vector at Thule for the classes of days of strong magnetic activity (solid line), of weak magnetic activity (dashes) and of average magnetic activity (dots-dashes)

A vector which has as its origin P_0 and which turns uniformly describes 24 elements corresponding to 24 hourly intervals on its hodograph. Beginning with the point P_0 , each of the elements is under an angle of 15° . Therefore the point P_1 which is at a distance of 10γ from P_0 in the direction corresponding to the n^{th} hourly interval as the origin.

Each element of the hodograph is seen from the point P_1 under an angle which is different from 15° . The difference is shown as a function of the hourly interval in figure 17. In the diagram where the direction of the vector as a function of the hourly interval is shown, the rotation seen from P_0 is uniform, therefore represented by a straight line (dotted in figure 18), and the rotation seen from P_1 is represented by a solid line. The maximum variance towards the west corresponds to the hourly interval n , and the easterly one to $n + 12$. The minimum intensity is always less than 30γ in all cases. A shift P_0P_1 in the direction of the minimum intensity corresponds to a variation of an angle of 7.5° (fig. 19). The angular variance due to an error of origin is therefore less than 15° . The variances measured are generally greater than 15° (see table 6) and the average variance is 53° . An error in the determination of the undisturbed field cannot, therefore, explain the lack of uniformity observed in the rotation, unless it were systematically directed according to the least intense vector, much greater than 10γ . No source of systematic error of

this sort was seen.

The general aspects of the curves 15.1, 15.2, 16.1 and 16.2 were resumed, assuming that the greater the modulus of the current vector, the closer its direction will be to that of the sun.

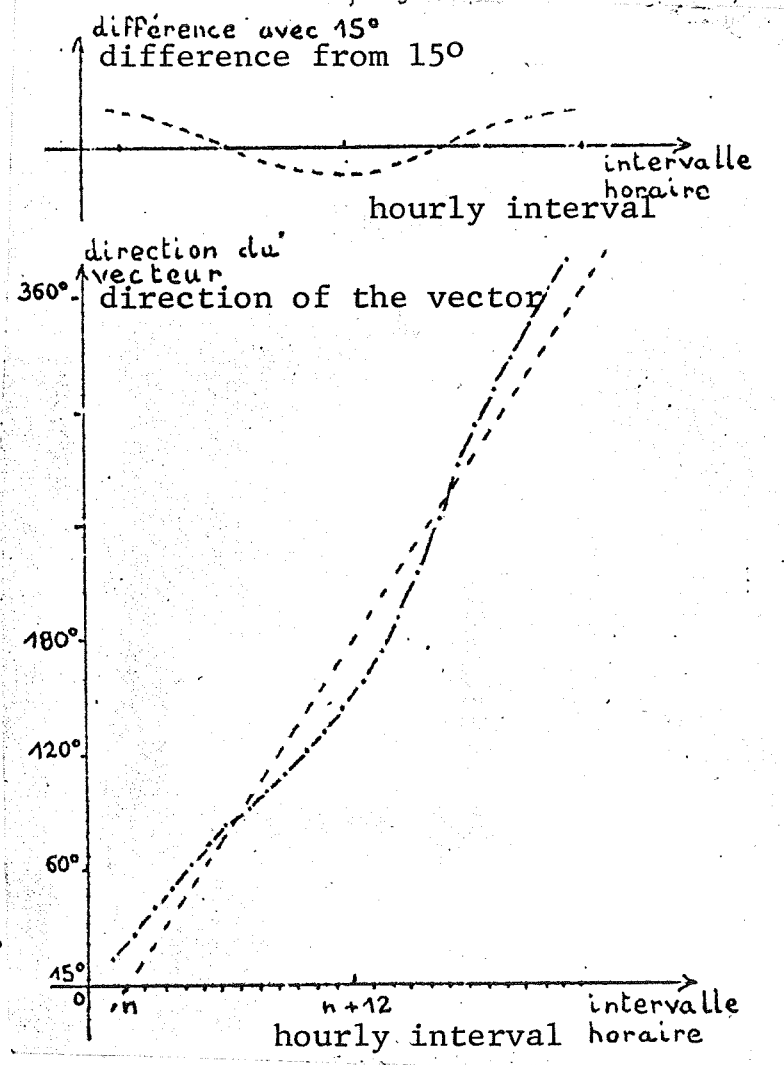


Fig. 17 and 18 Comparison of the uniform rotation seen from P_0 (----) and from P_1 (-.-.)

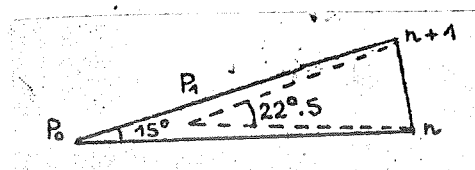


Fig. 19 Effect of the shift P_0P_1 in the direction of the vector of minimum intensity.

CHAPTER 4

Study of I

Notice the definition of the daily parameter I_j :

$$I_j = \frac{1}{24} \sum_{i=1}^{24} |i_{ij}|$$

Lebeau (1965) brought out a linear relation between the average value of the amplitude of the magnetic activity described by the local K indexes and the average value of corresponding I for the same station. This relation was established for Dumont d'Urville in 1958. The average values were taken from classes of days corresponding to the increasing values of I. Here the I parameter, day by day, the values taken for different stations were calculated. Good correlations lead to the consideration that I is a representative of phenomena at the planetary level. Hence, it was compared to A_p , planetary index of magnetic activity.

1. Calculation of I, effect of an error of origin:

The values of I in 1958 for the ten stations studied and for the station Little America (LA) were calculated. The uncertainty about I resulting from the uncertainty of the determination of the undisturbed field is evaluated by the average variance between the values of I calculated beginning with the origin of P_0 and beginning with the points P_E, P_N, P_W, P_S (Chapter 3, 1.1) The calculation was made by Vostok.

The average variance corresponding to P_E is 3.3γ ,

P_N of 3.3γ , P_W of 2.4γ , and P_S of 2.5γ . The average variance is 2.8γ . The average value I for Vostok is 92.1γ . The uncertainty about I is, therefore, on the order of 3%.

2. Comparison of the values of I for different stations.

The behavior of I as a function of two characteristic parameters of a given station, the magnetic colatitude and the geographic latitude will be made precise.

To isolate the eventual influence of the magnetic colatitude, the stations of the same latitude will be grouped together; this leads to the formation of two groups among the Antarctic stations. The stations Wilkes, D'Urville, Oasis, and Mirny are at a latitude close to 66° S and the stations Scott Base, Vostok and Little America are at a latitude near 78° S (see table 1). The stations will be compared two by two within both groups. Each day is represented by a point in the diagram where the I values relative to the station S_1 are assigned to the abscissa and those relative to the station S_2 are assigned to the ordinate (fig. 20 relative to Wilkes and Mirny). The average value of the proportion $\frac{IS_2}{IS_1}$ is calculated as the slope of the straight line of the least distances going through the origin drawn through these points. When three (or four) stations are used, each proportion $\frac{IS_2}{IS_1}$ can be compared

to $\frac{Is_2}{Is_3} \times \frac{Is_3}{Is_1}$ (and to $\frac{Is_2}{Is_4} \times \frac{Is_4}{Is_1}$). Note that, because of gaps in the observations, these different determinations concern groups of days which do not strictly overlap.

The values of the slopes of the straight lines and the values adopted for each proportion are assembled in Table 7.1 for the first group (the average value for the three determinations was taken) and in table 7.2 for the second group. (The two determinations yield identical results).

It is found that two stations belonging respectively to one or the other of the two preceding groups have the same magnetic colatitude; these are Wilkes and Scott Base. The values of \bar{I} will be assigned the value of 1 arbitrarily for these two stations and the value of \bar{I} for another station will be calculated by the proportion $\frac{\bar{I}}{IWk}$ for the first group and $\frac{\bar{I}}{ISB}$ for the second group (table 8).

The result is shown in figure 21 where the results thus reduced of I as a function of magnetic colatitude are shown. It is given that the average value of I augments as the magnetic colatitude of the station diminishes.

The group of stations available did not permit making the effect of geographic latitude precise in the same way. In fact only two stations, Wilkes and Scott Base are at the same magnetic latitude and at different geographic latitudes. The proportion

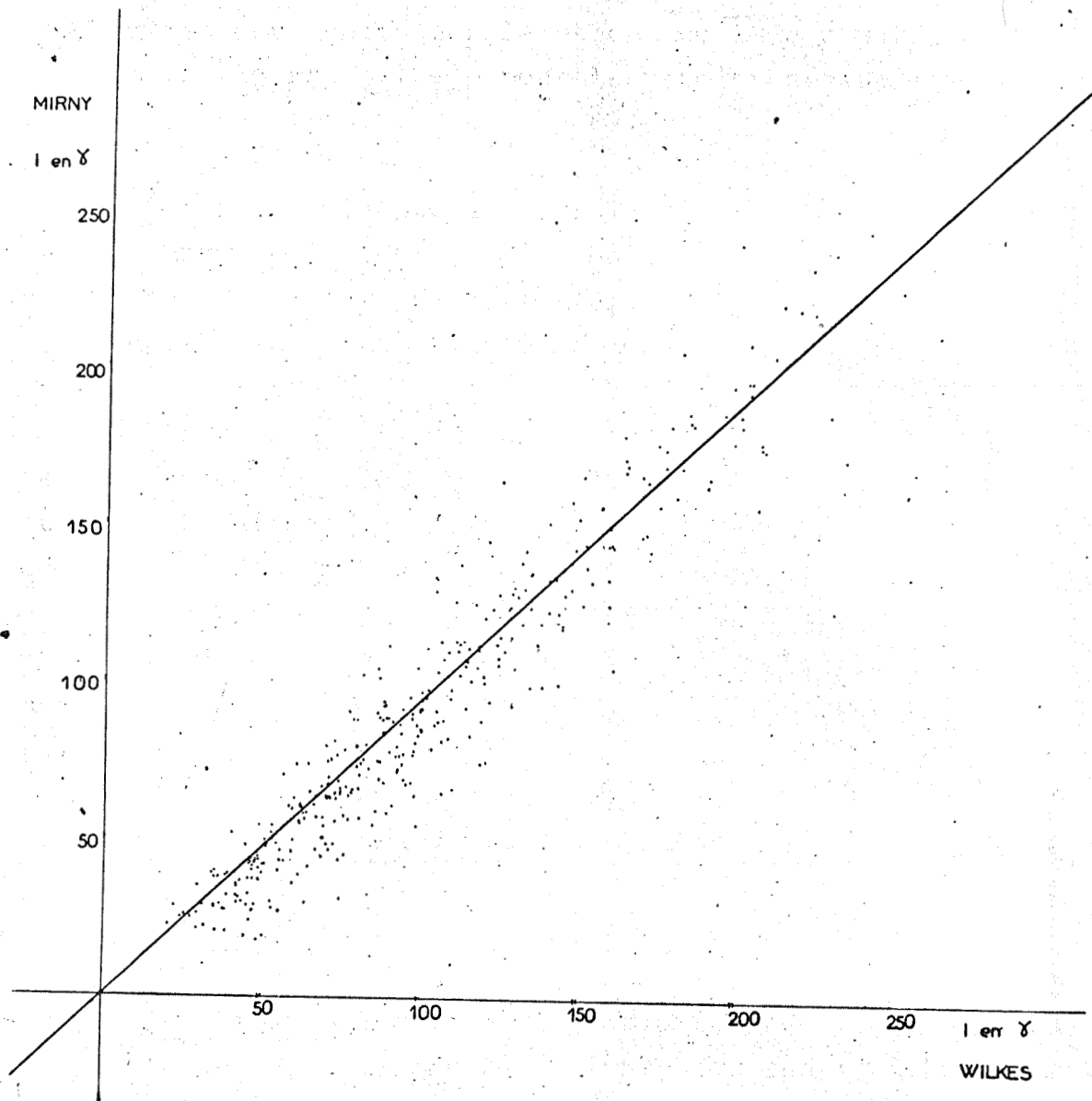


Fig. 20 $\frac{I_{mi}}{I_{wk}} = 0.936$. This average proportion was determined for the slope of the straight line of the least distances drawn through the points (I_{wk}, I_{mi}) .

Stations s ₁ et s ₂		$\frac{I_{s_2}}{I_{s_1}}$	s ₃	$\frac{I_{s_2}}{I_{s_3}} \times \frac{I_{s_3}}{I_{s_1}}$	s ₄	$\frac{I_{s_2}}{I_{s_4}} \times \frac{I_{s_4}}{I_{s_1}}$	Valeur moyenne Average value
DU	WK	1.056	OA	1.037	Mi	1.048	1.047
DU	OA	1.015	WK	1.034	Mi	1.006	1.018
DU	Mi	0.981	WK	0.988	OA	0.990	0.986
WK	OA	0.979	Mi	0.960	DU	0.961	0.967
WK	Mi	0.936	OA	0.954	DU	0.929	0.940
OA	Mi	0.975	WK	0.956	DU	0.967	0.966

Table 7 Values of average proportions $\frac{I_{s_2}}{I_{s_1}}$ for stations of the same latitude. 7.1 1st group DU, WK, OA, Mi (geographic latitude $\approx 66^\circ S$)

Stations s ₁ et s ₂		$\frac{I_{s_2}}{I_{s_1}}$
SB	Vo	1.012
SB	LA	0.788
Vo	LA	0.779

7.2 2nd group: Vo, SB, LA (geographic latitude $\approx 77^\circ S$)

Station	colatitude magnétique	reduced value of I Valeur réduite de I
Vo	5.50	1.012
DU	9.48	0.955
WK	9.83	1.
SB	10.04	1.
OA	11.61	0.967
Mi	13.18	0.940
LA	16.13	0.788

Table 8 Reduced values of I

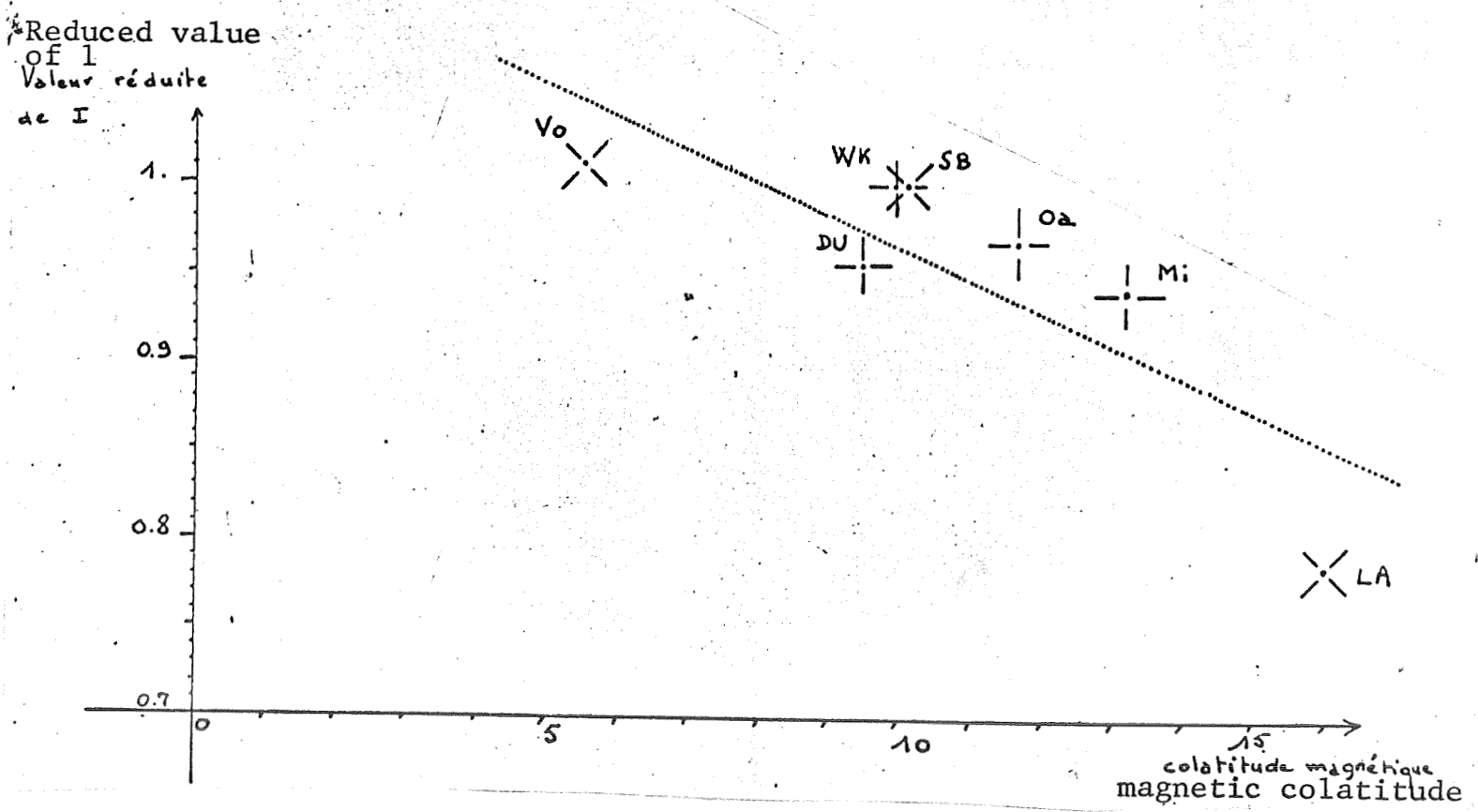


Fig. 21 Reduced values of I as a function of the magnetic colatitude. The straight line of the least squares was drawn.

of average yearly values of I , $\frac{IW_k}{ISB}$ is equal to 1.09, which indicates a weak increase of I with the geographic colatitude for the same magnetic latitude.

3. Evidences of seasonal variation:

3.1. Seasonal variation for an isolated station:

Figure 22 shows the variations of I as a function of months for the stations in the southern hemisphere: Wilkes, Mirny, Vostok and Scott Base. An annual cycle having its maximum in the summer is very apparent and the curves which correspond to the different stations are very comparable.

3.2 Compared variations of two stations:

To compare the seasonal variations of two stations the value of the average proportion $\frac{Is2}{Is1}$ will be calculated by the slope of the straight line of the least distances passing through the origin, passing through the points which represent the days of the months.

Between two stations of the same hemisphere, but of different latitudes, it was not possible to find a seasonal variation of the proportion $\frac{Is2}{Is1}$.

However, the comparison of two stations of different hemispheres brings out seasonal influences which are in phasic opposition. In figure 23 the seasonal variation of the proportion $\frac{IGO}{IMI}$ which brings out the inverse seasonal effects undergone by the I values relative to both stations is represented. The disconnection of the curve observed in December can be interpreted by the fact that the

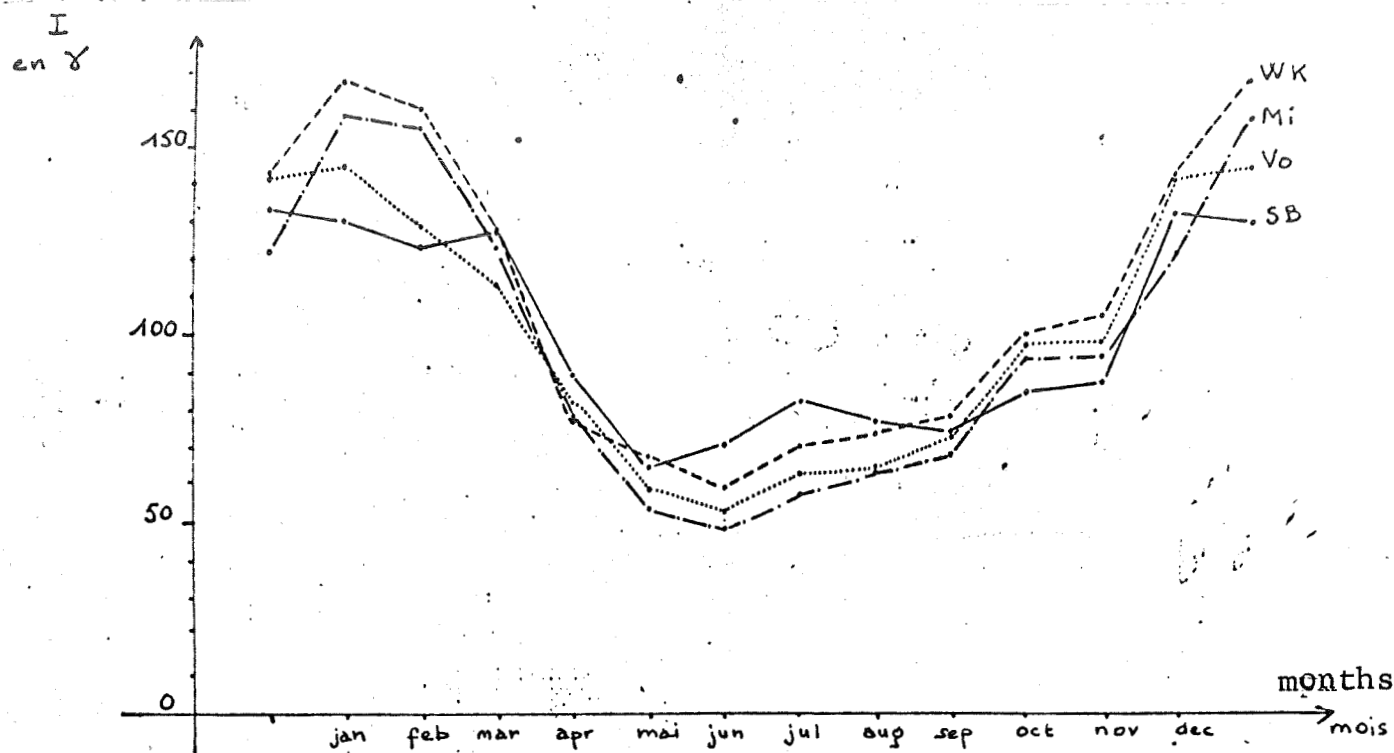


Fig. 22 Seasonal variation of I for Wilkes, Mirny, Vostok, and Scott Base

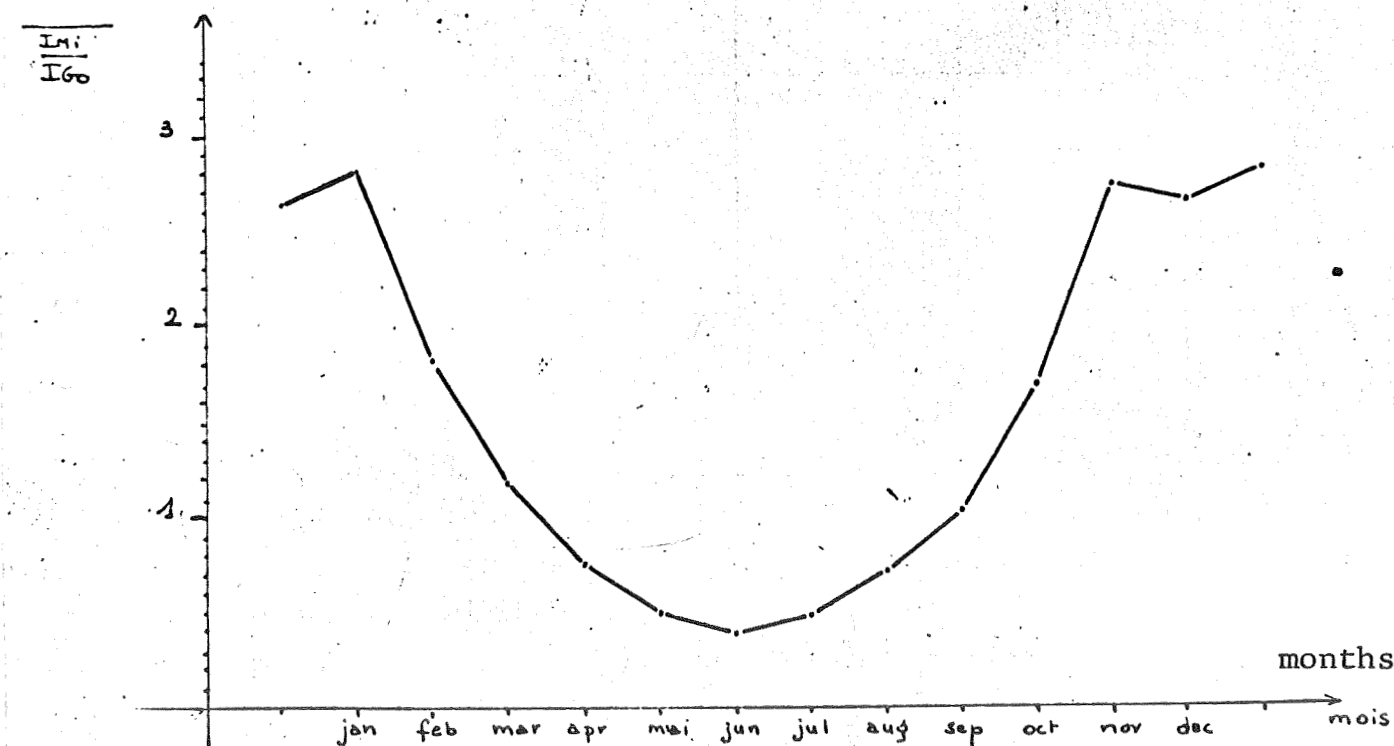


Fig. 23 Seasonal variation of the proportion $\frac{I_{mi}}{I_{go}}$ calculated by month.

sun was always below the horizon at Godhavn (latitude $69^{\circ}14'N$), the solar height no longer modulates the ionospheric conductivity (Lebeau 1965). There is no analagous effect in June at Mirny because it is at a lower geographic latitude ($66^{\circ}33'S$).

4. Comparison of I to Ap:

First an average annual relation between I and Ap (year 1958) will be established. Next a coefficient of seasonal variation will be introduced.

4.1 Average annual relation between I and Ap:

For the classes of days corresponding to the increasing values of Ap, the average value of I will be calculated.

For a given station, the average relation between I and Ap in 1958 is described by the curve drawn through the points $(\overline{Ap}, \overline{I})$, representatives of each class, in a diagram where Ap is assigned to the abscissa and I to the ordinate. The curves relative to the stations studied resemble each other (figure 24). Their slope decreases as Ap and I increase.

The curves will be represented as follows:

$$I = a Ap^{\alpha} \quad \alpha < 1$$

α and a are calculated by the slope and the ordinate at the origin of the straight line of the least squares in Y drawn through

the points ($\text{Log } \bar{A}_p$, $\text{Log } \bar{I}$) (figure 25)

$$\text{Log } I = \alpha \text{ Log } A_p + \text{Log } a.$$

The values of the slope and of the ordinate at the origin of this straight line for the different stations are assembled in table 10. It is given that the value of the coefficient α increases as the magnetic colatitude of the station increases, similarly the coefficient of proportionality decreases (figure 26).

This means on one hand that for a given value of A_p , I decreases at a greater rate in lower latitude stations than in the higher latitude stations.

The general phenomenon of expansion of the activity towards the lower latitudes is expressed here quantitatively for the interior of the auroral zone, where this occurs during a period of agitation, which is common in subauroral regions. The extension of this analysis towards the lower latitude regions should lead to values of α which approach unity, particularly in the observatories which will serve as a basis for the calculation of the A_p index, where α should equal 1.

4.2. Coefficient of seasonal variation:

To define the coefficient of the seasonal variation, the average value I_m of I was calculated for each month, as well as the average value of A_{p_m} of A_p . The previously established relation permits a correspondence between A_{p_m} and an average yearly value of I : $I(A_{p_m})$.

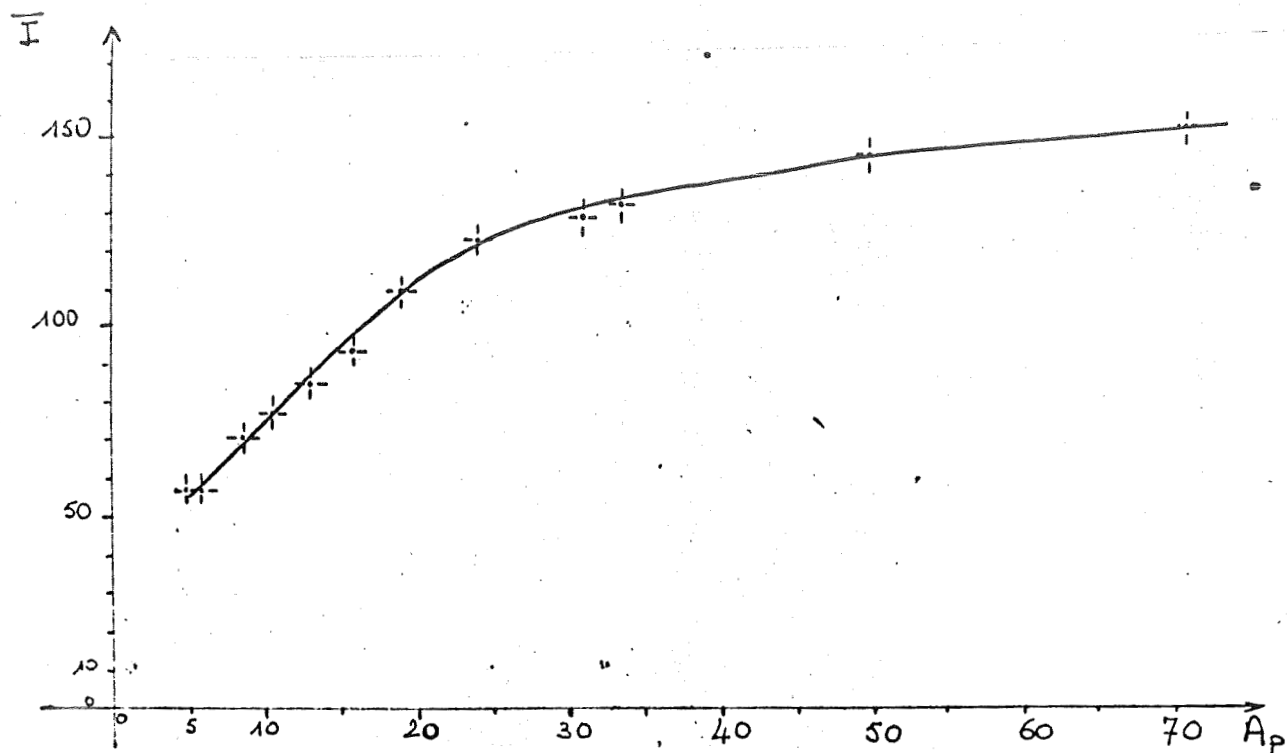


Fig. 24 Average yearly relation between A_p and the value of I at Oasis.

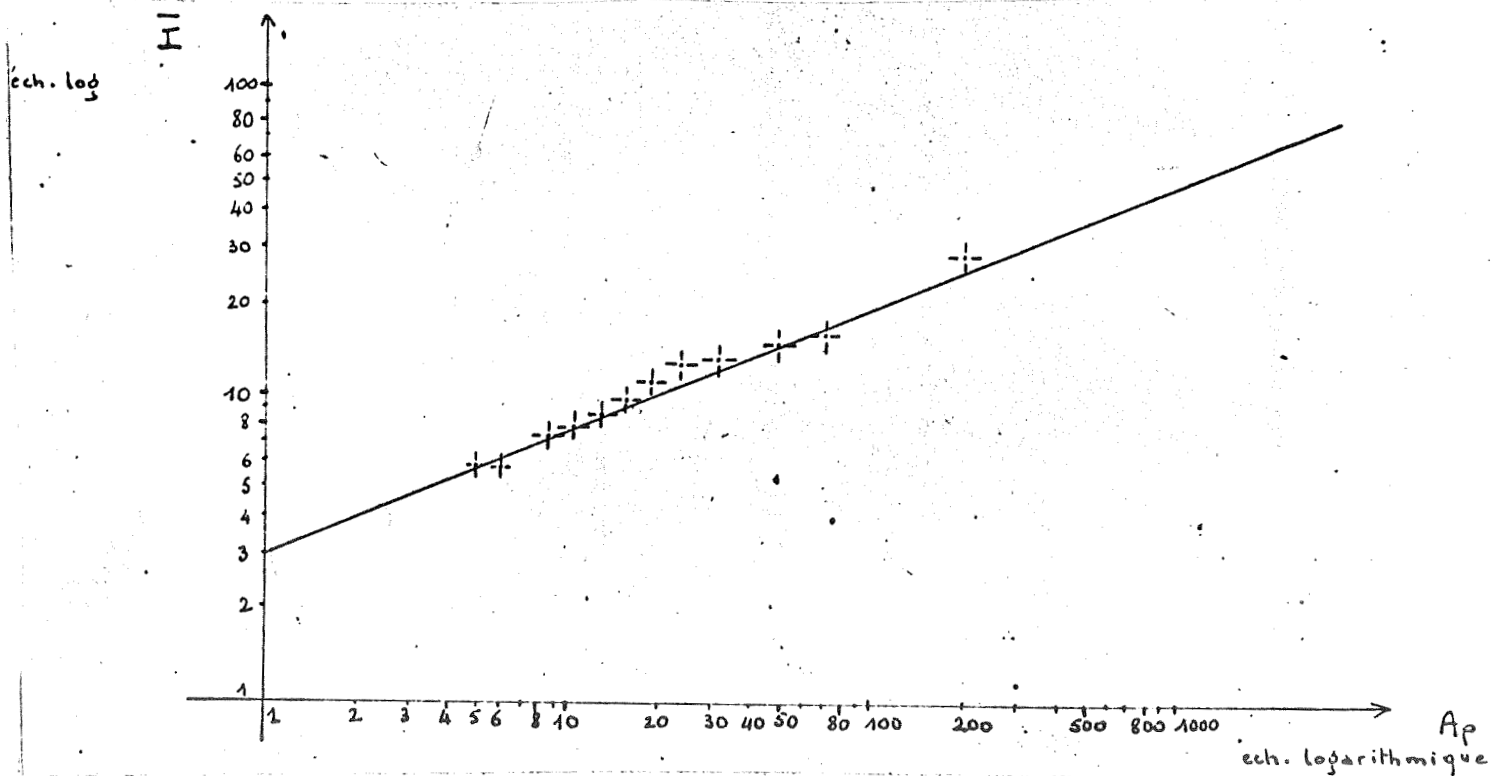


Fig. 25 Average yearly relation between $\text{Log } A_p$ and $\text{Log } I$ for Oasis.
The straight line of the least squares was drawn.
 $\text{Log } I = 0.41 \text{ Log } A_p + \text{Log } 30$

Classe	Ap included Ap compris entre et between and		Number of Nombre de jours	Average value Valeur moyenne de Ap en 1958 of Ap in 1958
1	2	6	71	4.79
2	5	7	63	6.06
3	7	10	77	8.52
4	9	12	70	10.50
5	11	15	66	13.05
6	13	18	66	15.58
7	16	23	65	19.05
8	19	31	69	24.03
9	23	48	66	30.74
10	27	200	70	50.34
11	7	14	126	10.02
12	15	26	98	19.31
13	27	47	44	33.34
14	48	131	24	69.08

Table 9

Station	Colatitude magnétique	α	a
Vo	5.50	0.321	38.20
DU	9.48	0.316	43.46
WK	9.83	0.354	40.00
SB	10.04	0.371	32.30
PO	10.19	0.366	38.60
Oa	11.61	0.408	30.01
Mi	13.18	0.440	27.44
Th	3.56	0.476	25.35
Gö	12.88	0.525	19.38

Table 10

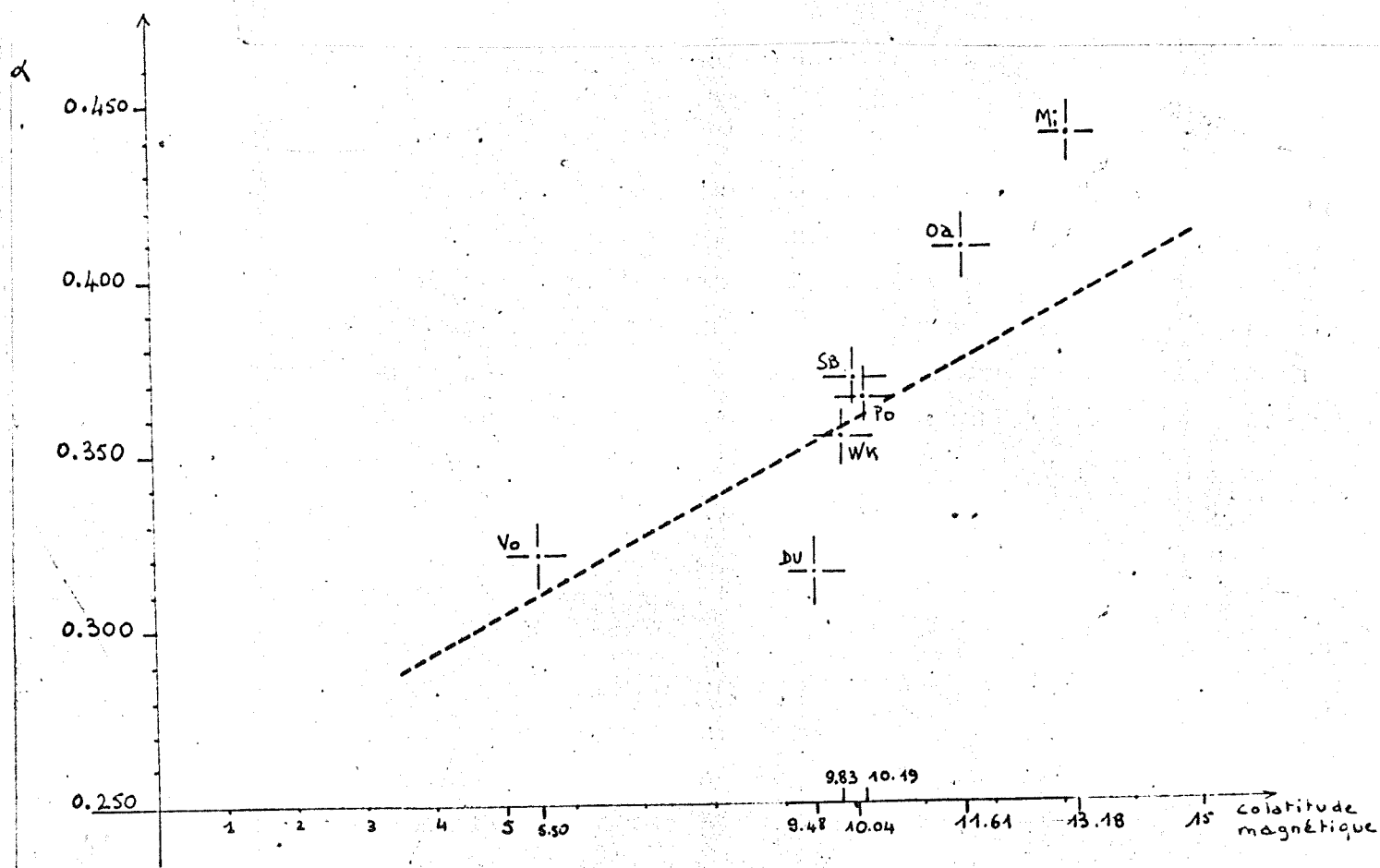


Fig. 26 The value of the coefficient α of the relation $I = aA^\alpha$ increases with the magnetic colatitude. The straight ^P line of the least squares was drawn through the points representing the Antarctic stations.

The seasonal variation of the coefficient:

$$k_m = \frac{I_m}{I(A_{p_m})}$$

for the year 1958 is represented in figure 27 for the different stations.

The difference of latitude between two Arctic stations on one hand and the seven Antarctic stations on the other, had no systematic influence on the coefficient of seasonal variation. The curves describe a maximum in summer and a minimum in winter. However, the average curve corresponding to the Arctic stations cannot be deduced from the corresponding average curve of the Antarctic stations by a simple shift of six months. Notice, though it cannot be explained, that its maximum estival is wider than the one corresponding to the Antarctic stations (figure 28).

4.3. Calculation of $A_p(I_j)$:

The correspondence between I and A_p is described, therefore, for a given station by a curve of seasonal variation and the yearly relation

$$I = a A_p^\alpha \quad (\S 4.1).$$

The daily coefficient of seasonal variation k_j is calculated by linear interpolation between the values of k_m corresponding to two successive months. From the yearly relation, $A_p(I_j)$ which is the value that A_p assumes when I is equal to $\frac{I_j}{k_j}$ can be deduced.

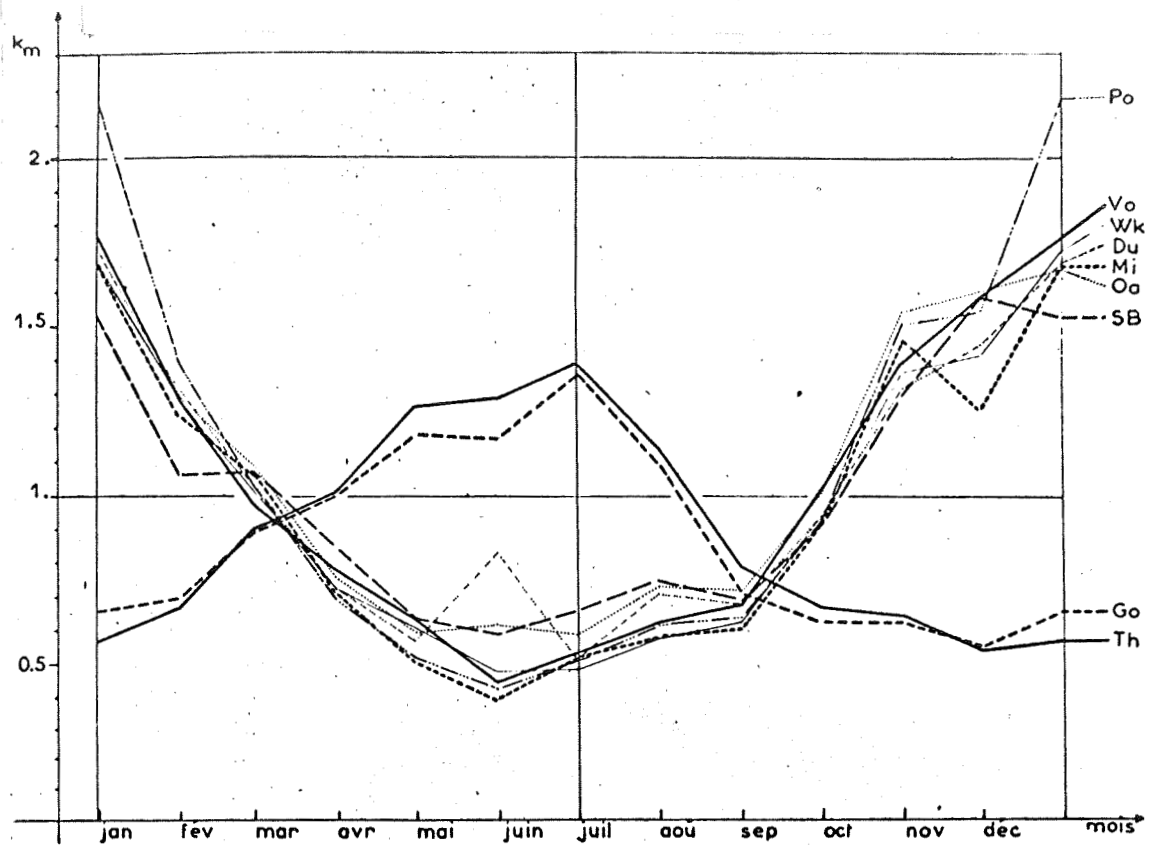


Fig. 27 Seasonal variation of the km coefficient for the stations studied.

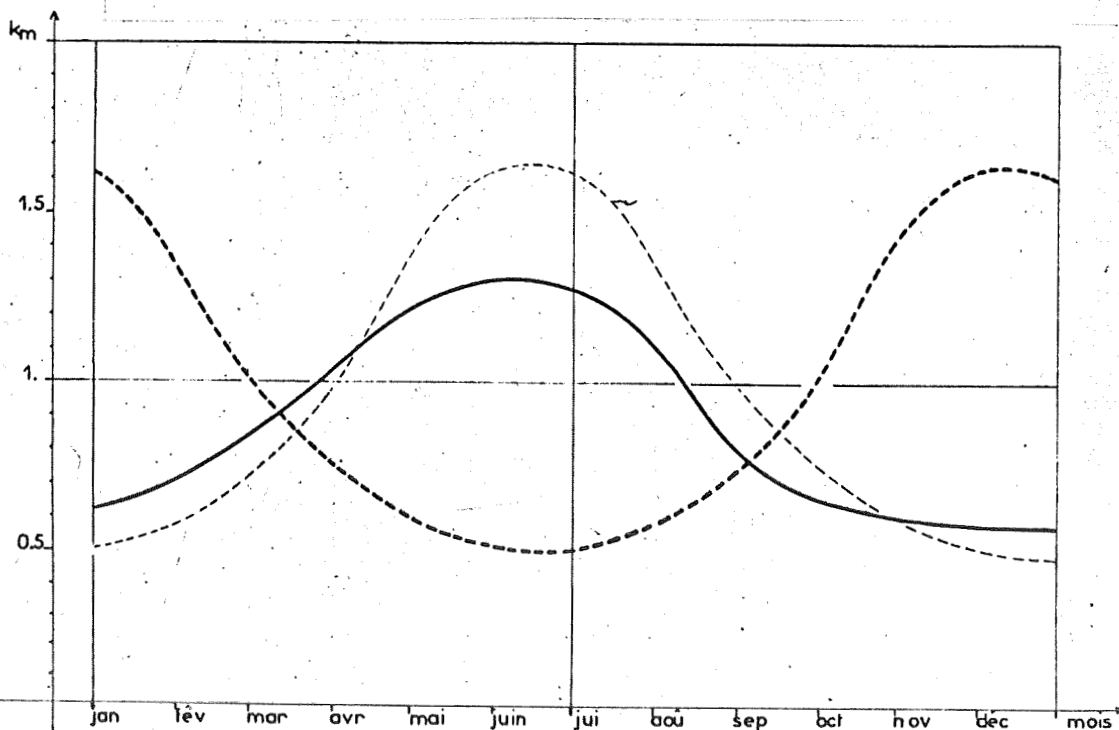


Fig. 28 Comparison of the average curves of seasonal variation for the Arctic stations (solid line) and the Antarctic station (dashes). They do not superimpose for a shift of six months.

To evaluate the finesse of these relations statistically established, the real value of Ap_j was compared daily to $Ap(Ij)$. It is given that, except for very agitated periods corresponding to local disturbances which are more or less acute, the variance between $Ap(Ij)$ and Ap_j is not greater than ± 5 .

The results of the relative calculations at Wilkes for the month of November and at Thule for the months of January, February, March and April will be given as examples (figure 29).*

Conclusion:

In this study the behavior of the hourly average values of the magnetic field in the very high latitude regions (magnetic colatitude $< 14^\circ$) was studied and their variation was interpreted as the effect of the electric currents circulating in the ionosphere.

This analysis was based on the concept of the undisturbed field and on the determination of local values of the undisturbed field. Two different methods lead to closely correlated results.

The daily maximum of the current density whose hour approaches local noon was established.

For the Arctic stations as well as for the Antarctic ones, the fact that the average direction of the currents is to the west of the direction of the sun was shown. The variance between these two directions is weak in a way that is directly proportional to the intensity of the currents. The average varies between 70° and 20° .

* See translator's note at end.

* The untranslated figure is supplied on next page

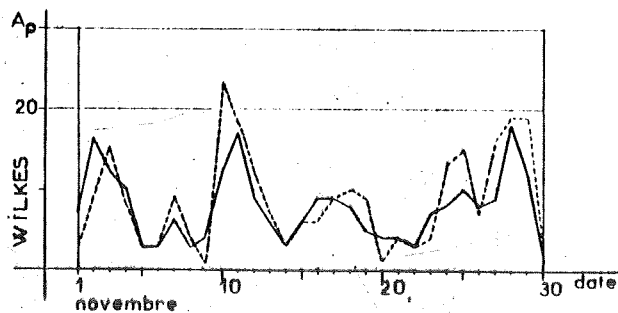
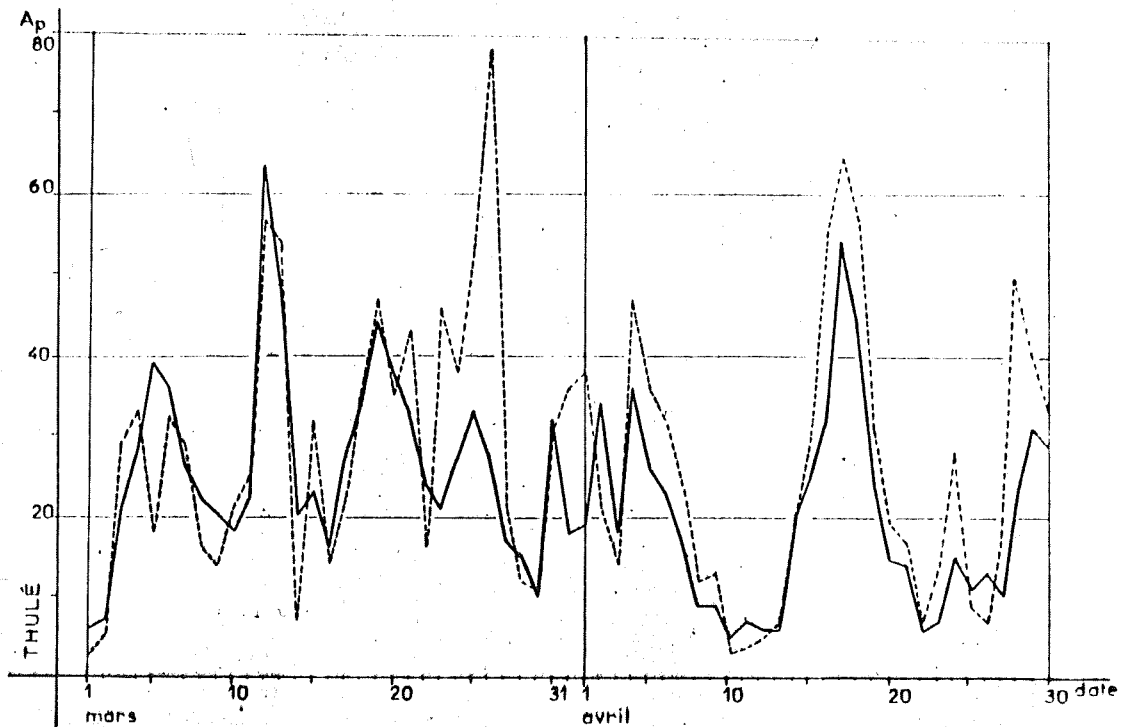
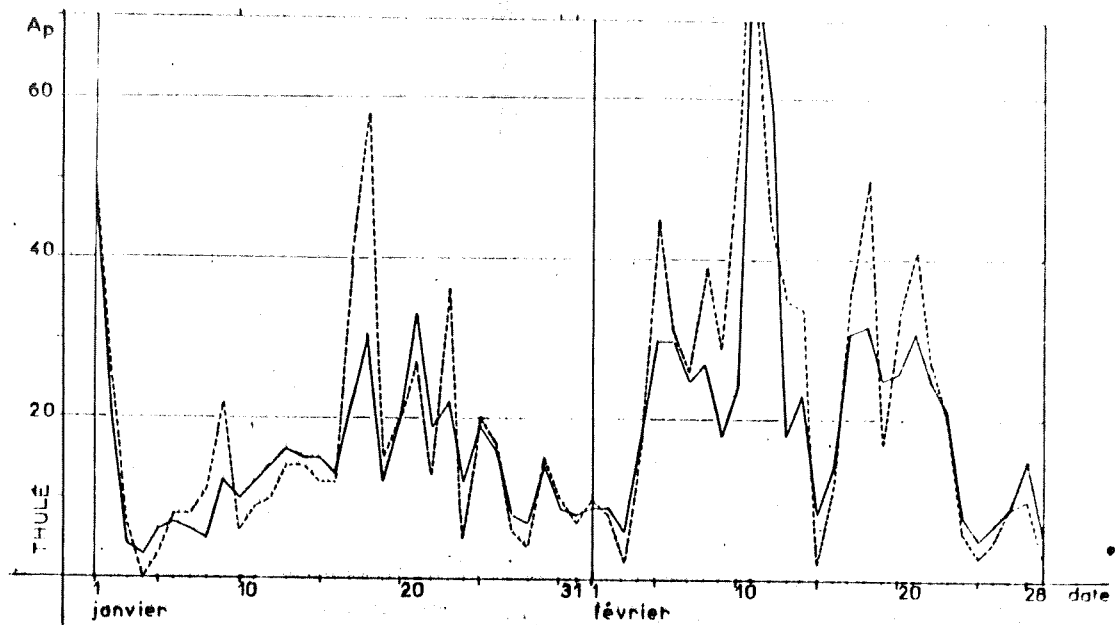


Fig. 29. Comparaison des valeurs journalières de A_p (II) (tireté) aux valeurs réelles de A_p (trait plein).

Next the average daily value of I of the intensity of the currents was studied; I possesses a seasonal variation of high amplitude ($\frac{I_{\text{winter}}}{I_{\text{summer}}} \approx 2.7$) which, in the same hemisphere, is only slightly influenced by the differences in geographic latitude; the average yearly value of I increases with the magnetic latitude. Likewise, I increases with A_p . It was established that the average yearly relation between I and A_p can be described by the equation:

$$I = a A_p^\alpha$$

where a and α are characteristic of a station; a increases with the magnetic latitude and α decreases. The latter property can be expressed quantitatively as an expansion of sheets of polar currents toward the lower latitudes as A_p increases. It would be interesting to research the problem of whether or not the behavior can be shown in the same way in auroral, subauroral and temperate regions.

Taking into account on one hand the seasonal variation and the relation between I and A_p on the other, it was shown that it would be possible to establish a value approaching A_p beginning with observed I .

Credits:

M. Lebeau directed and encouraged me for the duration of this work. I owe him an expression of my gratitude. I would not be able to cite all the members of GRI and of IPG, whom I

would like to thank for their aid and advice.

The calculations were made by the Numerical Calculation Service of the observatory of Meudon. I think particularly the operators of the night service, whose understanding often facilitated my work.

Appendix 1. The straight line of the shortest distances drawn through a cloud of points:

A straight line for which the sum of the squares of the Euclidian distances from the points of observation to the straight line would be minimal was searched. This quantity will be assigned D^2 .

It was shown that the minimal minimorum of D^2 is achieved when the origin is taken at the barycenter.

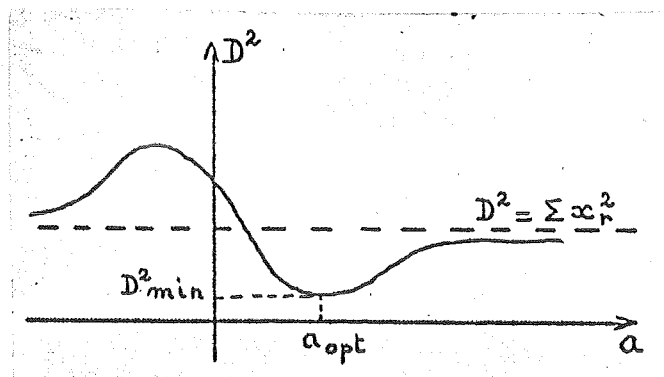
1. Calculation of D^2 - the origin is arbitrarily chosen:

N is the number of observation points; x_r , y_r are the coordinates of the points and d_r is the Euclidian distance of the point P_r at the straight line of the slope a , passing through the origin

$$d_r^2 = \frac{(y_r - ax_r)^2}{1 + a^2}$$

$$D^2 = \sum d_r^2 = \frac{a^2 \sum x_r^2 - 2a \sum x_r y_r + \sum y_r^2}{1 + a^2}$$

The variation of D^2 is studied as a function of a



D^2 is minimal when the value a_{opt} is taken

$$a_{opt} = -\frac{\sum x_r^2 - \sum y_r^2}{2} + \sqrt{1 + \left(\frac{\sum x_r^2 - \sum y_r^2}{2}\right)^2}$$

$$D_{min}^2 = \frac{\sum x_r^2 + \sum y_r^2}{2} - \sqrt{\left(\frac{\sum x_r^2 - \sum y_r^2}{2}\right)^2 + (\sum x_r y_r)^2}$$

2. Research of the minimum minorum of D^2 :

The coordinates of the points assigned to the origin taken at the barycenter are X_r, Y_r . The corresponding value of D_{min}^2 is represented as D_{b-min}^2 .

Beginning with the origin taken at $(\alpha, 0)$ the coordinates are:

$$x_r = X_r - \alpha$$

$$y_r = Y_r$$

which leads to:

$$\sum x_r^2 = \sum X_r^2 - N\alpha^2$$

$$\sum y_r^2 = \sum Y_r^2$$

$$\sum x_r y_r = \sum X_r Y_r$$

The value which corresponds to D_{min}^2 is represented by D_{a-min}^2 .

D_{b-min}^2 and D_{a-min}^2 are compared.

$$D_{b-min}^2 = \frac{\sum X_r^2 + \sum Y_r^2}{2} - \sqrt{\frac{(\sum X_r^2 - \sum Y_r^2)^2}{4} + (\sum X_r Y_r)^2}$$

$$D_{\alpha-\min}^2 = \frac{\sum X_r^2 + \sum Y_r^2}{2} + \frac{N\alpha^2}{2}$$

$$= \sqrt{\frac{(\sum X_r^2 - \sum Y_r^2)^2}{4} + \frac{N^2\alpha^4}{4} + \frac{2N\alpha^2}{4} (\sum X_r^2 - \sum Y_r^2) + (\sum X_r Y_r)^2}$$

It is easily seen that, whatever not nul, $D_{\alpha-\min}^2$ $D_{b-\min}^2$.
The straight line of the least distances passes through the barycenter.

Appendix 2 Data recorded on digital tape:

The average hourly values of the X (north) and Y (east) components of the horizontal components of the magnetic field were recorded on tape, on one hand for the 15 polar stations during 1958, and on the other for the station Godhavn for 15 years from 1950 to 1964. Each

Each station is designated by a code number of four figures that correspond to the number given to the station during the International Geophysical Year (Annals of the IGY 1964).

Station	Code numérique
Dumont d'Urville	1979
Wilkes	1977
Scott Base	1991
Godhavn	1049
Oasis	1976
Vostok	1996
Thulé	1021
Mirny	1978
Little America	1995
Mawson	1980
Byrd	1987
Macquarie Island	1961
Halley Bay	1989
Hallett	1988
Pionerskaya	1959

Each year of data is composed of 367 blocks of 49 words. The contents of each block are given in the following table.

block 1	Block of identification - Example: Identification of the data at Dumont D'Durville, 1958		
			Example
1st word	code number designation station		1979
2nd word	code of the definition of the magnetude recorded - the value of 7 corresponds to the x and y components		7
3rd word		year	58
4th word	date of the 1st day of year:	month	1
5th word		day	1
6th word	number of 1st day of the year, counted from		
	Jan. 1, 49, for years	49, 50, 51, 52	
	Jan. 1, 53, "	53, 54, 55, 56	
	Jan. 1, 57, "	57, 58, 59, 60	
	Jan. 1, 61, "	61, 62, 63, 64	366
7th word	number of successive days for which values are recorded		365
8th word to 49th word	42 time the value of 0		
block 2 to 366	365 daily blocks --even for the leap years (52, 56 60, 64) for which the correspondents for Feb. 29 were not given.		
1st word	0 if no observation is missing that day 1 if one or more observations are missing that day		
2nd word to 25th word	the 24 hourly values of X, the 1st corresponds to the first hourly interval: from 0 to the hour TU		
20th word to 49th word	The hourly values of Y		
block 367	Final block which will serve as test of positioning on the tape		
1st word	9999 (entire value)		
2nd word to 49th word	48 times the value of 0		

BIBLIOGRAPHY

Annals of the International Geophysical Year, 1964, Pergamon Press, Vol. 36.

BARTELS J., MECK N.H. et JOHNSTON H.F., 1939, The three-hour range index measuring geomagnetic activity. Terr. Magn., 44, 411 - 454.

BARTELS J., 1962, Collection of Geomagnetic Planetary Indices, IAGA, bulletin n° 18.

CHAPMAN S. et BARTELS J., 1940, Geomagnetism, Oxford.

FAIRFIELD D.H., 1963, Ionosphere current patterns in high latitude. J. Geophys. Res., 68, 3589 - 3602.

LEBEAU A., 1965, Sur l'activité magnétique diurne dans les calottes polaires, Annales de Géophysique 21, 167.

LEBEAU A. et SCHLICH R., 1962, Sur une propriété de l'activité magnétique diurne dans les régions de haute latitude (stations Charcot et Dumont d'Urville) C.R. Acad. Sc, 254, 1014 - 1016.

TRANSLATOR'S NOTE

Some confusion may exist in the use of sub letters and numbers, due to inconsistencies in the original French manuscript.

Reference is made to Fig. 29; however, there was no correspondingly numbered figure in the illustrations.